



A new approach for cultivating the cyanobacterium *Nostoc calcicola* (MACC-612) to produce biomass and bioactive compounds using a thin-layer raceway pond

Paula S.M. Celis-Plá^{a,b,*}, Tomás Agustín Rearte^{c,d}, Amir Neori^{e,f}, Jiří Masojídek^{g,h}, José Bonomi-Barufiⁱ, Félix Álvarez-Gómez^j, Karolína Ranglová^g, Jaqueline Carmo da Silva^k, Roberto Abdala^j, Cintia Gómez^l, Martín Caporgno^g, Giuseppe Torzillo^{m,n}, Ana Margarita Silva Benavides^{n,o}, Peter J. Ralph^p, Thaís Fávero Massocatoⁱ, Richard Atzmüller^g, Julia Vega^j, Patricia Chávez^j, Félix L. Figueroa^j

^a Laboratory of Aquatic Environmental Research, Center of Advanced Studies, University of Playa Ancha, 2581782 Viña del Mar, Chile

^b HUB-Ambiental, Vicerrectoría de Investigación Postgrado e Innovación, University of Playa Ancha, 2340000 Valparaíso, Chile

^c Departamento de Recursos Naturales y Ambiente, Facultad de Agronomía, Universidad de Buenos Aires, CABA, Av. San Martín 4453, 1417, Buenos Aires, Argentina

^d Consejo Nacional de Investigaciones Científicas y Técnicas (CONICET), Argentina

^e Morris Kahn Marine Research Station, Department of Marine Biology, Leon Charney School of Marine Sciences, University of Haifa, Israel

^f The Interuniversity Institute for Marine Sciences in Eilat, Israel

^g Institute of Microbiology of the Czech Academy of Sciences, Center Algatech, Novohradská 237 – Opatovický mlýn, Třeboň, Czech Republic

^h University of South Bohemia, Faculty of Science, Branišovská 1760, České Budějovice, Czech Republic

ⁱ Botany Department, Center of Biological Sciences, Federal University of Santa Catarina, 88040-970 Florianópolis, Santa Catarina, Brazil

^j Universidad de Málaga, Instituto de Biotecnología y Desarrollo Azul (IBYDA), Facultad de Ciencias, Campus, Teatinos s/n E-29071, Málaga, Spain

^k Department of Botany, Center of Biological Studies, Federal University of Sao Carlos, Sao Carlos, Brazil

^l Department of Chemical Engineering, University of Almería, Carretera Sacramento s/n, 04120, Almería, Spain

^m CNR – Institute of Bioeconomy, Via Madonna del Piano, 10, I-50019 Sesto Fiorentino, Italy

ⁿ Centro de investigación en Ciencias del Mar y Limnología (CIMAR), Universidad de Costa Rica, San Pedro de Montes de Oca 2060, Costa Rica

^o Escuela de biología, CIMAR – Centro de Investigación en Ciencias del Mar y Limnología, Universidad de Costa Rica, San Pedro, Costa Rica

^p Climate Change Cluster, University of Technology Sydney, 123 Broadway, Australia

ARTICLE INFO

Keywords:

Aquaculture

Biochemical composition

In-vivo chlorophyll a fluorescence

Nostoc

Photosynthesis

Thin-layer raceway cultivator

ABSTRACT

The culture of microalgae and cyanobacteria in open systems has been improved through the novel approach of thin-layer raceway ponds. The importance of studying mass cultivation of the cyanobacterium *Nostoc calcicola* (further as *Nostoc*) lies in its biotechnological potential as a source of bioactive compounds for food and non-food applications. These compounds include polysaccharides, mycosporine-like amino acids and phycocyanin. *Nostoc* was cultured outdoors in a thin-layer raceway pond where the biomass production, physiological status, photosynthetic activity, and biochemical composition were monitored through the experimental period of 5 days. The biomass, as did the maximal quantum yield of PSII, maximal electron transport rate (ETR_{max}) and photosynthetic efficiency (α_{ETR}) increased throughout the experimental period showing the optimal operation of the thin-layer raceway ponds, due to the light penetrates deeper into the thin culture layer and thus more light is available to the cells. Oxygen levels in the culture increased over time, but no photoinhibition was evident indicating optimal action of non-photochemical mechanisms. *Nostoc* increased the total internal carbon content over the experimental period. Chlorophyll increased, whereas the N compounds such as the biliprotein phycocyanin decreased. Among the UV-absorbing compounds, polyphenols, mycosporine-like amino acids, such as shinorine and other unknown UV-A absorbing compounds were detected. These components showed a positive correlation to antioxidant activity. Thus, the optimal accumulation of biomass and the accumulation of bio-active compounds having antioxidant capacity show the possible biotechnological applications of *Nostoc*.

* Corresponding author at: Laboratory of Aquatic Environmental Research, Center of Advanced Studies, University of Playa Ancha, 2581782 Viña del Mar, Chile.
E-mail address: paulacelispla@upla.cl (P.S.M. Celis-Plá).

1. Introduction

The *Nostocaceae* are cosmopolitan family of Cyanobacteria which includes 40 species and 10 varieties [1]. These species can fix atmospheric nitrogen in the absence of combined nitrogen [2,3]. The filaments of the *Nostoc* spp. consist of photosynthetic cells with some N_2 -fixing heterocysts. The filaments are embedded in a protective gelatinous matrix made of polysaccharides and other organic substances [4].

Cyanobacteria show a great diversity of metabolic pathways which have evolved to adapt to varied environmental conditions, such that they are one of the most prolific microorganisms producing bioactive compounds [5]. Species from the *Nostocaceae* are an abundant source of bioactive compounds, including the polysaccharide k-carrageenan (k-car) [2], phycocyanin [6], auxins [7], as well as compounds that provide elevated antibiotic activity [8]. The gelatinous matrix is also effective at bio-absorbing metals [9].

Most biotechnology applications of cyanobacteria have been in the pharmacological and nutraceutical field [10]. Recently, there is great research interest concerning skin protection to substitute organic UV screening substances by biological UV photoprotectors, due to their negative effect of UV on human health, such as endocrine disruption properties [11], skin penetration [12], low photostability, low biodegradability and lack of effectiveness in skin protection [13]. In addition, commercial particulate UV filters (both inorganic and organic) are non-biodegradable [14]. UV photoprotectors with antioxidant capacity such as mycosporine-like amino acids and Scytonemin have been reported in *Nostoc* [15,16] and exopolysaccharides (EPS) [17].

Due to its use in food, feed and high-value compounds in the cosmetic industry, there is growing interest in the outdoor mass culturing of cyanobacteria, including *Nostoc* strains [18]. Mass cultivation of these species have a few challenges, for example, filamentous *Nostoc* strains are sensitive to friction caused by pumps used for culture circulation. Therefore, the most suitable outdoor cultivation systems production of biomass of *Nostoc* specie is open raceways or airlift

photobioreactors. However, the biomass volumetric productivity in open raceways is limited by the light availability inside the culture, due to the depth of the water column (10–30 cm). Increasing the daily integrated cell irradiance using thin-layer culture units is a promising approach [19]. These units provide a high ratio of surface area to total volume (S/V) and enable – due to suspension turbulence and short light path – rapid light/dark cell cycling, which improve photosynthetic performance [20]. Thin-layer cascades (TLCs) have been used successfully in the production of some microalgae, such as *Chlorella* spp. with extremely high productivity, *i.e.*, 14–52 g DW $m^{-2} d^{-1}$ [21,22]. Unfortunately, as mentioned above, these systems are not suitable for *Nostoc* species due to damage from pump circulation. Therefore, a novel thin-layer raceway pond (TL-RWP) design was employed here, where 1.5–2.5 cm layer of culture was circulated using a paddle wheel [19].

Varying outdoor growing conditions trigger a diverse range of photo-acclimation responses such as complex-regulation, high light attenuation in high cell density culture as well as spatial-temporal heterogeneity within the culture, all of which hamper optical assessment of photosynthetic health of the culture [23,24,21,25].

Optical monitoring techniques based on physiological behavior and photosynthetic activity of the cells are an important tool used to understand the photo-acclimation processes in outdoor cultures and there are crucial for their optimization. Pulse amplitude modulated (PAM) fluorimeters using saturating pulse analysis of quenching can measure photosystem II (PSII) quantum yield and other important variables [26,27]. Quantum yields measured *in vivo* by chlorophyll *a* fluorescence is related to quantum yields by O_2 evolution and CO_2 fixation [28,29], *i.e.*, linear relation between gross photosynthesis by O_2 evolution and electron transport rate (ETR) determined by *in vivo* chlorophyll *a* (Chl*a*) fluorescence. The linear relation is not maintained under certain conditions such as elevated irradiance which is result in the consumption of oxygen by Mehler reaction [28] or nutrient deficiency [30]. ETR has been also used to estimate algal biomass productivity [22]. The relative electron transport rate (rETR) is determined by using values of the

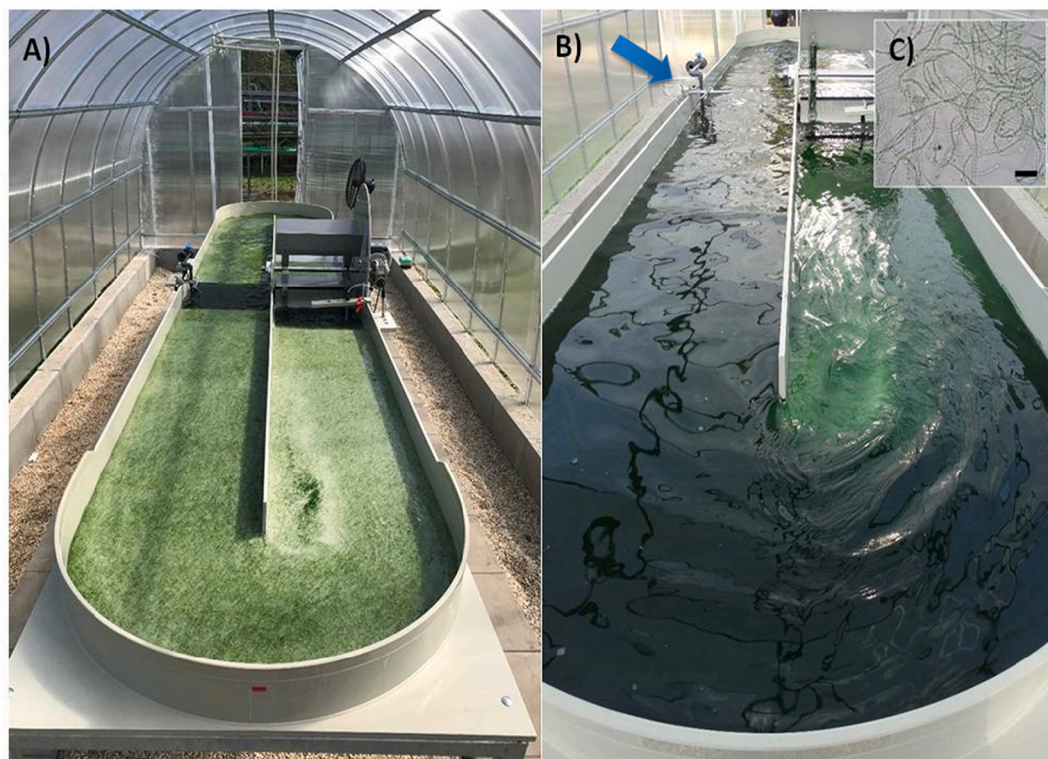


Fig. 1. Thin-layer raceway pond after the inoculation on day 1 (panel A) and at the end of cultivation trial on day 5 (panel B) with the detailed microscopic picture (panel C, magnification 600 \times).

effective quantum yield of PSII (Yield II) and simultaneously measuring the incident irradiance (E) between 400 and 700 nm (photosynthetic active radiation, PAR) [31]. However, the light absorption, the fraction of cellular Chla in PSII, its associated light-harvesting complex (LHCII (FII)), and the fraction of absorbed quanta to PSII (fAQ_{PSII}), should also be measured simultaneously to calculate the absolute ETR and consequently their relation to biomass productivity [32, 22]. Cyanobacterial fluorescence responses when measured by PAM instruments differ from microalgae due to structural and functional properties of the photosynthetic apparatus [33]. Cyanobacteria usually exhibit lower quantum yield of PSII based on fluorescence measurement, due to interference caused by fluorescence emitted from the phycobilisomes in the light harvesting antennae associated with the photosynthetic electron transport chains, as well as differences in state transitions [34].

In this study, the thin-layer raceway pond was used for the cultivation of cyanobacteria. The biomass production, photosynthetic activity and biochemical composition of an outdoor culture of *N. calcicola* (further abbreviated as *Nostoc*) were monitored during a 5-day outdoor trial. The physiological status and photosynthetic activity of the *Nostoc* culture were determined by *in-situ* PSII Chla fluorescence. Various *in-situ* and *ex-situ* Chla fluorescence technique and protocols were performed to estimate photosynthetic activity and productivity. The evaluation of methodologies used to determine biomass productivity, determination of the midday photoinhibition through real time to the maximal quantum yield of PSII (F_v/F_m), optical light absorption and effective quantum yield of PSII (Yield II) under different diurnal conditions, were the main objectives of these trials during the GAP10 workshop of Group of Aquatic Primary Productivity linked to International Limnology Society (ISL) entitled "Aquatic productivity - in the Omics Era", which was held in Třeboň (Czech Republic) between 19 and 30 August 2017.

2. Material and methods

2.1. Strain and culture growth conditions

The trials were performed at the Center Algatex in Třeboň, Czech Republic (48°59'15"N; 14°46'40"E). The cyanobacterium *Nostoc calcicola* strain MACC-612 was obtained from the Culture Collection of Szechenyi István University in Mosonmagyaróvár, Hungary. The seed culture was grown in an 80-litre laboratory photobioreactor in an inorganic growth medium using internal white LED illumination [BG-11 medium, [35]] at 30 °C for 10 days. The *Nostoc* culture was inoculated to a thin-layer raceway pond (TL-RWP; manufactured by F&M srl., Firenze, Italy) at an initial biomass concentration of about 0.18 g DW L⁻¹ and was grown for 5 days (22 to 26 August 2017) (Fig. 1A-C). The unit has a surface area of 5 m², a culture volume of 120 L and the S/V ratio of 40 m⁻¹. The TL-RWP unit was housed in a polycarbonate greenhouse with ventilation by electrical fans and heaters to maintain cultivation conditions (Fig. 1A day 1–Fig. 1B day 5 of the trial). As the paddlewheel was placed in a sump, a thin culture layer between 1.5 and 2.5 cm could be maintained with a flow speed of about 0.2 m s⁻¹ (Fig. 1). Carbon dioxide was automatically added into the culture, based on pH regulation (8 ± 0.2).

2.2. Biomass (dry weight)

The measurement of biomass density was measured in triplicate once a day in the morning at 08:00 h, after evaporation compensation as described previously [36]. Dry weight of the biomass was measured by filtering 5 mL of cyanobacterium culture on pre-weighted microfiber filters (Whatman GF/F, glass microfiber filter). The filters were dried in an oven at 105 °C for 8 h, cooled down (10 min) in a desiccator and re-weighed. The specific growth rate $\mu = (\ln X_2 - \ln X_1)/\Delta t$ [d⁻¹] was calculated over the cultivation period.

2.3. Bio-optic: light absorption measurement

In-vivo spectral absorption of the cyanobacterium cells was measured and compared by two different techniques, in suspension [37] and on filter [38,39].

The *Suspension Technique* (ST) was performed in a double-beam scanning spectrophotometer (Shimadzu UV3000, Kyoto, Japan) using 1-cm cuvettes filled with culture samples, which were collected at 3 sampling times (08:00, 14:00 and 17:00 h) and diluted with fresh medium to obtain an optical density lower than 0.8. To minimize the effect of light scattering from the cell surface, the sample cuvette was placed close to the detector window of the photomultiplier tube and a light diffusor (printer paper) was placed in between. Specific optical absorption (or attenuation) cross-sections of the suspension [$a_{sus(\lambda)}$, (m⁻¹)] were calculated from the spectral absorption measurements (400–750 nm):

$$a_{sus(\lambda)} = 2.303 * OD_{sus(\lambda)} * 100 \quad (1)$$

where $OD_{sus(\lambda)}$ is the optical density of the suspension at a determined wavelength (corrected for absorbance at 750 nm), 2.303 is the conversion factor from log₁₀ to ln, and 100 is the conversion from cm to m. This value was divided by the Chla content of the sample, expressed in mg m⁻³, to provide the Chla specific absorption cross-sections [a_{sus}^* , (m² mg⁻¹ Chla)].

The *Quantitative Filter Technique* (QFT) was performed in an integrating sphere spectrophotometer, where samples were collected at 2 sampling times: at 11:00 and 17:00 h. To measure $OD_{filter(\lambda)}$ 1–2 mL of samples (depending on the biomass concentration), was filtered onto GF/F filters. The same volume of culture medium was filtered and used as a blank. Specific absorption cross-sections of the filter [$a_{f(\lambda)}$, (m⁻¹)] were calculated from the spectral absorption measurements (400–750 nm):

$$a_{f(\lambda)} = \frac{2,303 * [aOD_{filter(\lambda)} + bOD_{filter(\lambda)}^2]}{(V/A)} \quad (2)$$

where $OD_{filter(\lambda)}$ is the optical density of the filter at a determined wavelength (corrected for absorbance at 750 nm), V is the volume filtered (m³) and A is the area (m²) of filtration; in this way V/A determines the same path length as that of the suspension. The variables *a* and *b* in the equation (Eq. (2)) were estimated from the correlation of the $OD_{sus(\lambda)}$ vs $OD_{filter(\lambda)}$, using a second-order polynomial function and corresponds to the amplification factor (β) [38]. Chlorophyll specific absorption cross-section [$a_{f(\lambda)}^*$, (m² mg⁻¹ Chla)] was calculated by dividing the specific absorption cross-sections of the filters by the Chla concentration of the samples, expressed in mg m⁻³. For the estimations of absolute ETR, the average value of chlorophyll specific absorption cross-sections (a_{sus}^*) in the range from 400 to 700 nm were used.

2.4. Irradiance and temperature measurements

Outdoor irradiance (PAR, $\lambda = 400$ –700 nm) and ultraviolet radiation (UVA, $\lambda = 315$ –400 nm) and temperature (°C) were monitored during the trial each 15 min by using data logger (Zippo-Hobbo-U12-UV) with the PAR sensor (SQ-12) and a UVA sensor (LPUVA01, Apogee Instruments, USA) [40].

Inside PAR irradiance, in the culture was determined by an immersed mini-spherical quantum sensor (US-SQS, H. Walz GmbH, Germany) located at 2 cm depth (Fig. 1B).

2.5. In-vivo chlorophyll a fluorescence method

The *in-vivo* Chla fluorescence was determined by several pulse amplitude modulated (PAM) fluorometers.

1) *Junior PAM* (Walz GmbH, Germany) was used for *in-situ/on-line* measurements in the outdoor raceway. Chl fluorescence data was recorded each 5-min throughout the day using saturating pulse analysis of fluorescence quenching. The plastic fiber optics (100 cm, 1.5 mm diameter) was submerged in the first 5 mm of the water column in the culture surface of the raceway (arrow Fig. 1B), together with a spherical PAR quantum sensor (US-SQS, Walz GmbH, Germany). These two sensors provided simultaneously Chl fluorescence and PAR irradiance measurements, respectively, as described previously [41,42]. Blue light-emitting diodes (LED, 460 nm) in the control box were powered by PC via a USB interface and provided measuring actinic light and saturating pulses. WinControl-3 software was used for data acquisition and recording (Fig. 1B - blue arrow). The *in situ* relative electron transport rate (rETR) rate through PSII was determined as follows:

$$rETR_{in\ situ} = \Delta F/F_m' \times E_{PAR} \quad (3)$$

where $\Delta F/F_m'$ is the effective quantum yield of PSII being $\Delta F = F_m' - F_t/F_m$ (when F_t is the basal fluorescence), E_{PAR} is the incident photosynthetically active irradiance [43]. Although rETR is frequently associated with biomass productivity, it is a relative value and should be cautiously considered since photo-biochemical responses depend on the absorbed light and not on the incident irradiance [44].

2) *Water PAM* (Walz GmbH, Germany) and PAM 2100 (Walz GmbH, Germany) were used to measure rapid light response curves (RLCs) and determine the maximal quantum yield of PSII under laboratory conditions, *ex situ*. The Water PAM uses red light (654 nm) for saturation light pulses and actinic light and FR-LEDs for exciting PSI (740 nm), whereas PAM 2100 uses red light (654 nm) for saturation light pulses and actinic light and FR-LEDs for exciting PSI (735 nm). The measurements were conducted in dark-adapted samples (triplicate), which were collected at four times during the day (08:30, 11:00, 14:00 and 17:00 h).

Maximal quantum yield of PSII (F_v/F_m) was calculated as the ratio of variable fluorescence ($F_v = F_m - F_0$) to maximal fluorescence (F_m) in dark adapted culture samples (fully oxidized reaction centers). F_0 is the basal fluorescence of fully oxidized reaction centers (dark - adapted algae) and F_m is the maximal fluorescence after application of saturating light pulse of $>4000 \mu\text{mol photons m}^{-2} \text{s}^{-1}$. A low intensity modulated measuring light (LEDs of a peak wavelength at 650 nm; $<0.3 \mu\text{mol photons m}^{-2} \text{s}^{-1}$, frequency of 0.5–1 kHz) which does not induce photosynthetic activity, was used to measure basal fluorescence (F_0). As in cyanobacteria, the fluorescence was emitted by the phycobilisomes light harvesting antenna and since photosynthesis and respiration share the plastoquinone (PQ) pool, it is difficult to measure real minimum fluorescence F_0 , thus different protocols were used for this purpose:

- (1) *DCMU Method*. The 'true' F_m was determined under low actinic illumination ($\sim 150 \mu\text{mol photons m}^{-2} \text{s}^{-1}$) in the presence of 10^{-5} M DCMU [3-(3,4-dichlorophenyl)-1,1-dimethylurea] which blocks the electron transport beyond the PSII complex. In the dark and after addition of the electron transport inhibitor DCMU, the PQ pool is oxidized and the apparent value in dark-adapted *Nostoc* MACC-612 cultures is usually 15%–20% lower than the 'true' F_m [45]. When illuminated, the reaction centers are reduced.
- (2) *FR-Dark-R-FR*. According to Hanelt et al. [45], a sequence of far red light (FR, time = 5 s, and irradiance = $30 \mu\text{mol photons m}^{-2} \text{s}^{-1}$), followed by the dark period for 5 min, then red light (R, time = 5 s, irradiance = $8 \mu\text{mol photons m}^{-2} \text{s}^{-1}$), and finally FR (time = 5 s and irradiance = $30 \mu\text{mol photons m}^{-2} \text{s}^{-1}$) was applied.

Rapid light curves (RLC) and Electron transport rate (ETR). The absolute electron transport rate (ETR) was determined after a series of eight 20-s light exposure periods using stepwise increasing irradiances of red light in the Water PAM ($E_1 = 77$, $E_2 = 115$, $E_3 = 166$, $E_4 = 253$, $E_5 = 373$, $E_6 = 570$, $E_7 = 846$ and $E_8 = 1220 \mu\text{mol photons m}^{-2} \text{s}^{-1}$) to generate a RLCs. The ETR was calculated according to Jerez et al. [22] as follows (Eq. (4)) with the addition of the a_{sus}^* variable:

$$ETR = \Delta F/F_m' \times E_{PAR} \times a_{sus}^* \times fAQ_{PSII} \quad (4)$$

where a_{sus}^* ($\text{m}^2 \text{mg}^{-1} \text{Chl}$) is the chlorophyll specific absorption cross-section determined by the suspension method and fAQ_{PSII} is the fraction of absorbed quantum to PSII. The value of fAQ_{PSII} was 0.3 for cyanobacteria according to Johnsen and Sakshaug [43]. The maximal ETR (ETR_{max}) as estimator of photosynthetic capacity, the initial slope of ETR vs irradiance curves (α_{ETR}) as an estimator of photosynthetic efficiency, irradiance at saturation (E_{kETR}), and irradiance for the initial photoinhibition (Eopt), was obtained from the tangential function as reported by Eilers and Peeters [46].

Non-photochemical quenching (NPQ) as an estimate of energy dissipation was calculated according to Bilger et al. [47] and Celis-Plá et al. [48] (Eq. (5)), and the maximal NPQ (NPQ_{max}) values were obtained directly from each RLC fitting, according to [46].

$$NPQ = (F_m - F_m')/F_m' \quad (5)$$

The yield of non-photochemical losses, $Y(NO)$ and $Y(NPQ)$ were determined according to Kramer et al. [49] and Hendrickson et al. [50]. The variable $Y(NO)$ (Eq. (6)) is the fraction energy passively dissipated as heat and fluorescence, mainly due to closed PSII reaction centers. High $Y(NO)$ values indicate an inability to protect the cell from photo-damage by excess radiation [51].

$$Y(NO) = F_t/F_m \quad (6)$$

$Y(NPQ)$ (Eq. (7)) is the fraction of energy dissipated as heat via regulated photo-protective NPQ mechanisms.

$$Y(NPQ) = (F_t/F_m') - Y(NO) \quad (7)$$

2.6. *In situ* dissolved oxygen measurement

The rate of oxygen production (RO_2) *in-situ* in the TL-RWP was calculated according to Doucha and Lívanský [52]. The build-up of dissolved oxygen (DO) was estimated by the relative differences in DO between two measuring points, one right after the paddlewheel and the second 9.6 m downstream (before the paddlewheel). The net rate of oxygen production (RO_2) by the culture was calculated from the differences in DO concentration between these two points, considering the mass transfer of oxygen between the suspension and the atmosphere, given constants such as water temperature and an average estimate of turbulence, using the following formula:

$$R_{O_2,DOmean} = \left(\frac{uh}{L}\right)(C_{O_2,L} - C_{O_2,0}) + K_{L,O_2}(C_{O_2,mean} - C_{O_2}^*) \quad (8)$$

where $R_{O_2,DOmean}$ is the mean rate of oxygen production by microalgae per 1 m^2 of culture area ($\text{g O}_2 \text{ m}^{-2} \text{ h}^{-1}$); u = velocity of suspension flow on culture area (720 m h^{-1}); h = thickness of the suspension layer across culture area (0.0225 m); L = distance between DO concentration measurement points (9.6 m); $C_{O_2,L}$ and $C_{O_2,0}$ = DO concentrations ($\text{g O}_2 \text{ m}^{-3}$) at sampling points, respectively; $K_{L,O_2} = 0.2 \text{ (m h}^{-1})$ represents mass transfer coefficient for oxygen; $C_{O_2,mean}$ = average DO concentration in culture ($\text{g O}_2 \text{ m}^{-3}$); $C_{O_2}^*$ = DO concentration in equilibrium with ambient oxygen concentration ($\text{g O}_2 \text{ m}^{-3}$). The first part of the equation represents DO concentration increase along the flow path of the culture, and the other part of the equation expresses mass transfer of oxygen between the algal culture and the atmosphere, depending on the DO concentration gradient and water temperature.

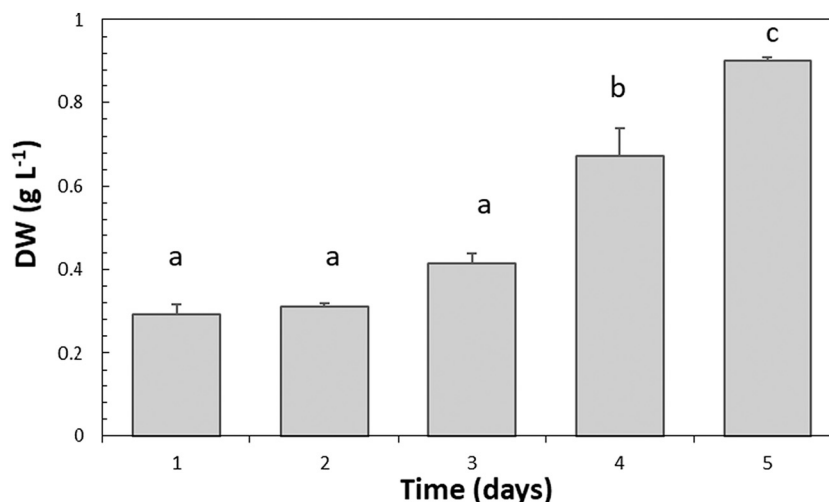


Fig. 2. Biomass density expressed in g DW L⁻¹ during the trial in the culture of *Nostoc calcicola* grown in a thin-layer raceway pond. Biomass density was determined twice a day in the morning (08:00 h) and in the afternoon (17:00 h). Results are expressed in a percentage as means \pm standard deviation (n = 3).

In the model proposed by Barceló-Villalobos et al. [53], the oxygen production was estimated according to the oxygen accumulation along the flow path of the culture, the mass transfer along that path and in the sump of the paddlewheel and finally normalized to the surface area.

was expressed as equivalent of Starch (% Starch) by multiplying by a factor of 0.9 according to Kumar and Prabhasankar [56]. Total protein content was estimated using the N-Protein conversion factor (4.78) for cyanobacteria and microalgae according to Lourenço et al. [57]. Lipids

$$RO_{2,mean} = \frac{Q_{liq}([O_2]_{end} - [O_2]_{beg}) + K_{La,channel}([O_2]_{mean} - [O_2]^*)V_{channel} + K_{La,PW}([O_2]_{mean} - [O_2]^*)V_{PW}}{A} \quad (9)$$

where the Q is the flow rate (m³ h⁻¹), $K_{La,channel}$ and $K_{La,PW}$ are the mass transfer coefficients for the flow path of the culture (0.9 h⁻¹) and paddlewheel (164 h⁻¹), respectively, $V_{channel}$ and V_{PW} are the volume (m³) of the channel and paddlewheel respectively, and A is the area (m²) between the starting and end measuring points.

2.7. Biochemical compounds

2.7.1. Nutritional status, internal carbon (C) and nitrogen (N) concentration

The total content of internal carbon and nitrogen in microalgae samples were determined by an elemental analyzer (CNHS 932, Michigan, USA) according to Celis-Plá et al. [42].

2.7.2. Pigment content

For Chl assay, 5 mL of samples were collected in glass tubes and centrifuged at 2600 \times g for 8 min and then the pellets were re-suspended in 80% acetone. The cells were disrupted using a vortex mixer for 2 min with glass beads (diam. 1 mm) and centrifuged afterwards. The extraction step was repeated until the pellet was colorless. The absorbance of collected supernatants was measured using a high-resolution spectrophotometer (UV 2600 UV-VIS, Shimadzu, Japan; slit width of 0.5 nm) and the concentration of Chl (mg mL⁻¹) was calculated according to Wellburn [54]. The content of Phycocyanin was determined according to Kursar et al. [55] and was expressed in mg DW g⁻¹.

2.7.3. Carbohydrates, proteins, lipids and fatty acids

Quantification of soluble carbohydrates was spectrophotometrically determined by the Anthrone method [56]. To obtain a standard curve, D-Glucose was used at final concentrations of 10–100 mg L⁻¹. The result

were quantified spectrophotometrically using Sulfo-Phospho-Vanillin (SPV) method [58]. To obtain the standard curve for lipid determination, triolein was used in concentrations of 0.1–0.6 mg L⁻¹. To obtain the fatty acid profile, the lipids were trans-esterified [59]. They were dissolved in 1 mL of toluene with butylated hydroxytoluene (BHT) (50 mg L⁻¹) and 2 mL of 1% of sulfuric acid in methanol. 3.5 mL of ultrapure water and 4 mL of the mixture of Hexane and Diethyl ether (1:1) with 0.01% of BHT, was vortexed and centrifuged (2000 \times g for 5 min), the liquid part was divided into two phases. The maximum weight of about 80 mg of lipids was used for determination. The tubes were flushed with N₂, incubated in a bath at 50 °C and kept in darkness for 16 h. 3.5 mL of ultrapure water and 4 mL of the mixture of Hexane and Diethyl ether (1:1) with 0.01% of BHT, was vortexed and centrifuged (2000 \times g for 5 min), the liquid part was divided into two phases. The upper part was transferred to another tube, shaken with 1.5 mL of KHCO₃ (2%) and centrifuged (2000 \times g for 5 min), and the liquid part was divided into two phases again. The upper layer was transferred to another tube and evaporated with N₂. The fatty acid methyl esters (FAMES) present in the tube were dissolved in 1–2 mL of Hexane and filtered through a Sep-Pak Aminopropyl (NH₂) cartridge in another pre-weighed tube. The Hexane part, that contained the fatty acids, was evaporated again and the tubes were weighted and fatty acid mass present in the sample was calculated. Finally, 40 mg of FAMES per mL of hexane were analyzed by gas chromatography (Focus GC, Thermo Scientific).–

2.7.4. Mycosporine-like amino acids, phenolic compounds, and antioxidant activity

The mycosporine-like amino acids (MAAs) were analyzed by HPLC (Waters 600) as described in [60], and the phenolic compounds were spectrophotometrically determined following [42,48], where a standard curve was prepared by using phloroglucinol. Finally, the antioxidant

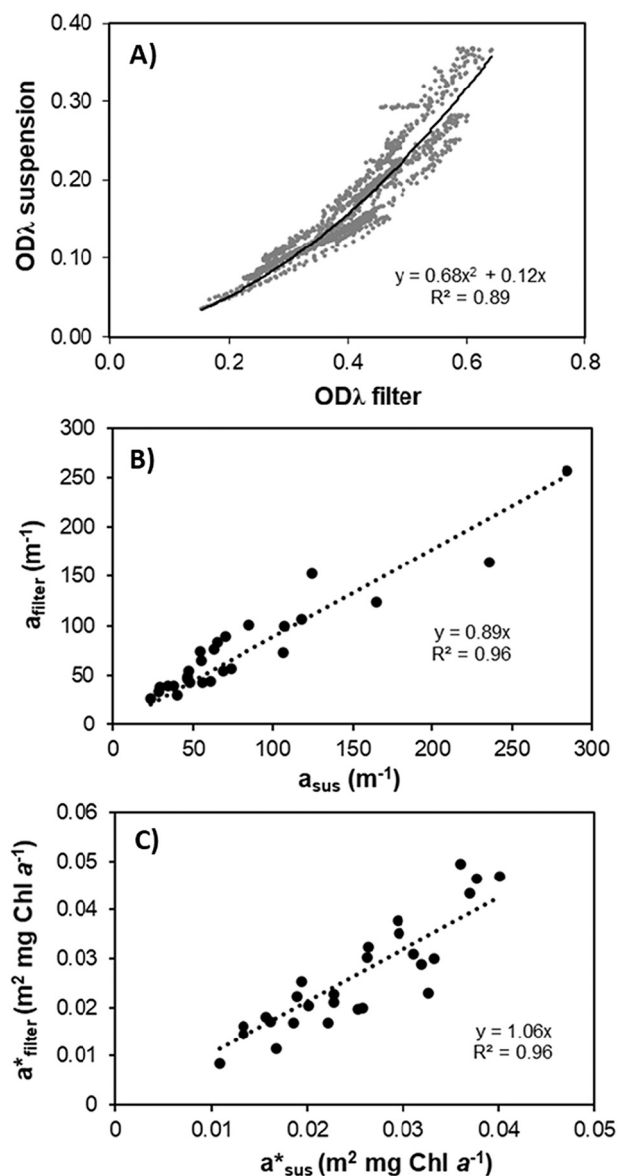


Fig. 3. *In-vivo* absorption measurements. A) Spectral optical density of suspension ($OD_{\lambda, \text{sus}}$) as a function of spectral optical density of filter ($OD_{\lambda, \text{filter}}$), B) Relationship between specific absorption cross-sections measured by QFT method (a_{filter}) and that measured by suspension method (a_{sus}) expressed as attenuation coefficient (m^{-1}) and C) Relationship between specific absorption cross-sections measured by QFT method (a_{filter}^*) and that measured by suspension method expressed in chlorophyll-specific absorption cross-sections ($\text{m}^2 \cdot \text{mg Chl a}^{-1}$).

activity was evaluated by the ABTS [2,2'-azino-bis (3-ethylbenzothiazoline-6-sulfonic acid)] method according to [61]. The reaction was completed after 8 min at laboratory temperature and the absorbance was measured at 413 nm. A calibration curve was prepared using a concentration range (0–30 μM) of Trolox.

2.8. Statistical analysis

The data were presented as the average \pm standard error ($n = 3$, SE). The effects of treatments on the different variables were evaluated using the analysis of variance (ANOVA) [62]. Student-Newman-Keuls (SNK) *post hoc* tests were performed for significant ANOVA interactions and are shown in the figures as lower-case letters when applicable. Homogeneity of variance was tested using Cochran tests and by visual inspection of the

residuals [62]. Analyses were performed by using SPSS v.21, (IBM, Endicott, New York, USA). The general variation patterns between physiological and biochemical variables measured in *Nostoc* were explored using a multivariate approach. A Principal Coordinates Analysis (PCA) was performed for this purpose based on Euclidean distance using PERMANOVA+ within PRIMER v.6 software package [63]. Each one of the variables was represented by an arrow in the ordination plot pointing to the samples displaying the highest amount of that compound. Pearson correlation coefficients were calculated and tested between all measured dependent variables using Sigma plot 14.0 (Systat software, Slough, Berkshire, UK).

3. Results and discussion

The incident outdoor PAR irradiance reached maximal values close to 2000 $\mu\text{mol photons m}^{-2} \text{s}^{-1}$ and UVA radiation 60 W m^{-2} at midday (at 13:00 CEST) (Fig. S1). The local weather was mostly dominated by thin clouds on some days in the afternoon. The second day (23 August 2017) was a clear-sky day. The air temperature in the greenhouse varied from 15 to 20 $^{\circ}\text{C}$ at night and maximal values were 25–40 $^{\circ}\text{C}$ during the day (Fig. S1). Light is one of the most critical 'substrates' for microalgal production, as the growth rate depends on its availability within the cultivation system [64]. Indeed, during the trial, the maximal incident irradiance reached 2000 $\mu\text{mol photons m}^{-2} \text{s}^{-1}$, but the irradiance intensity inside the culture in the TL-RWP was between 200 and 800 $\mu\text{mol photons m}^{-2} \text{s}^{-1}$ due to the light attenuation by the water column and cyanobacterium biomass. In the thin-layer systems, which are comprised of various compartments, cells can experience a wide range of light levels, because of the different light penetration among different sections, the light regime and culture densities [65,66]. The biomass density (g DW L^{-1}) increased significantly along with the culture; the biomass increased with the days as tap water was added in the morning to compensate for evaporation ($p < 0.05$; Fig. 2, Table S1). The growth optimization can influence the biomass productivity and biomass composition. The biomass density was 0.3 g L^{-1} and reached 0.9 g L^{-1} , which corresponds to the growth rate doubled in the second half ($\mu = 0.28 \text{ d}^{-1}$) of the experiment.

3.1. Light absorption and photosynthetic activity

The light absorption results measured by the QFT correlated well with the suspension technique (Fig. 3). The light attenuation obtained by the filter ($OD_{(\lambda)}_{\text{filter}}$, normalized to cm^{-1}), was higher than the light attenuation of suspension ($OD_{(\lambda)}_{\text{sus}}$) due to reflection and scattering on the filter; therefore, the path length amplification factor (β) was higher than one (~ 2.6). When the blue spectral range, the amplification factor was lower than values observed at red spectral range. To estimate the absorption cross-section of the suspension using filter data, the relationship between $OD_{(\lambda)}_{\text{filter}}$ and $OD_{\lambda, \text{sus}}$ (400–700 nm) was fitted to a simple quadratic equation (Fig. 3A) according to [67,38,68]. The final equation was $a_{f(\lambda)} (\text{m}^{-1}) = 2.303 [0.12OD_{\text{filter}(\lambda)} + 0.68OD_{\text{filter}(\lambda)}^2]/(V/A)$. The corrected values of absorption on the filter were compared with those obtained from the suspension (Fig. 3B and C). The linear relation ($R^2 = 0.96$) between specific absorption cross-sections measured by QFT method (a_{filter}) and by suspension method (a_{sus}) expressed as attenuation coefficient (m^{-1}) (Fig. 3B) and as chlorophyll specific absorption cross-sections ($\text{m}^2 \text{ mg Chl a}^{-1}$) (Fig. 3C) was observed. A good estimation for the chlorophyll specific absorption cross-sections (a^*) was observed since the slope was close to one (slope = 1.06, see Fig. 3C).

The relationship between photosynthetic activity and growth implies the determination of the quanta absorbed by the cells (*i.e.*, absolute ETR) and it correlate to biomass productivity (*i.e.*, $\text{g DW L}^{-1} \text{ d}^{-1}$) [22,39]. Both photophysiological and biochemical responses do not depend on the incident irradiance, but the absorbed and utilized quanta. Estimation of light absorption is a complex process, due to the wave-particle duality of light: the diverse light interaction phenomena with cells, such as

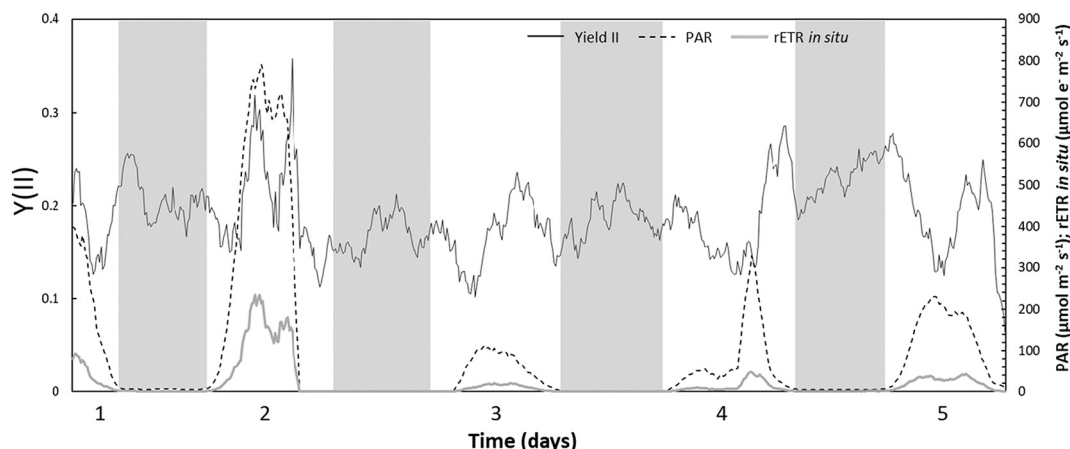


Fig. 4. Effective quantum yield (YII) during the day period and maximal quantum yield (F_v/F_m) measured in the dark in the *Nostoc calcicola* culture were monitored every 5 min using Junior-PAM (continues line), PAR irradiance (dashed lines), expressed as $\mu\text{mol photons m}^{-2} \text{s}^{-1}$ determined by a spherical PAR mini-sensor connected to Junior PAM and Relative electron transport rate (rETR) expressed in $\mu\text{mol electrons m}^{-2} \text{s}^{-1}$ (continuous lines).

scattering, absorption and diffraction are explained by the wave description, whereas the particle nature of light influences fluorescence [69]. Determination of the absorption coefficient can be performed by several optical methods. The QFT technique is a widely extensively used method for determination of absorption coefficient with phytoplankton populations in oceanography [70,71,72], while the suspension technique is used mainly for microalga cultures [44].

The difference observed can be attributed to the different spectrophotometer devices used: a spectrophotometer with an integrated sphere was used for the QFT technique whereas [38] used a single-beam spectrophotometer. The absorption coefficient values (a and a^*) estimated here by both methods were quite similar, with both linear regression slopes close to 1, in contrast to the higher slope (1.98) obtained by [39]. Therefore, both methods could be used to perform absorption measurements with *Nostoc* cultures. The β factor (path length amplification factor by the filter) can vary depending on the species and wavelength. We observed an average β factor of 2.64 ± 0.33 across the different experimental days, and it varied slightly with wavelength (it was lower in blue as compared with red region). The β factor obtained was within the range reported by [71] of 2.43–4.71 for several species.

The effective quantum yield of PSII (YII) measured *in-situ* showed variation throughout the day which was related to irradiance in the culture (Fig. 4). The Y(II) decreased from the morning to midday and then increased towards evening on most days as it is usual in outdoor cultures [73]. The highest irradiance inside the culture was found on day 2 ($800 \mu\text{mol photons m}^{-2} \text{s}^{-1}$), and Y(II) was inversely related to the maximal daily irradiance, as it decreased from 0.3 in the morning to 0.18 in the afternoon (Fig. 4). After dusk, the values of the actual PSII quantum yield Y(II) present a small increase and after about 4 h in darkness, it slightly decreased except for the last day 5 of the experiment (Fig. 4). Due to the variation in Y(II) and in the irradiance throughout the day, rETR showed large differences between the day with high irradiance on day 2 and the rest of the experimental time. The maximal values of rETR on day 2 were about $210 \mu\text{mol e}^- \text{m}^{-2} \text{s}^{-1}$ whereas in the rest of the days was less than $50 \mu\text{mol photons m}^{-2} \text{s}^{-1}$ (Fig. 4).

The average of the maximal quantum yield of the PSII (F_v/F_m) measured *ex-situ* increased throughout the experimental period (Fig. 5, Table S1). On the first day of the trial, various procedures were followed to determine F_v/F_m . The application of FR-Dark-R-FR before the saturation pulse determined values of F_v/F_m close to 0.2, whereas the application of DCMU reached values of about 0.3 (Fig. 5B). The application of only 10 min of dark reached much lower values, *i.e.*, 3 times lower than that of FR-Dark-R-FR treatment. Thus, FR-Dark-R-FR and DCMU treatments were applied and the rest of the experiment to

determine F_v/F_m . On day 2, from morning to afternoon, the F_v/F_m varied from 0.2 to 0.5, on day 3 from 0.3 to 0.55, on day 4 from 0.45 to 0.62, and on day 5 from 0.55 to 0.65 (Fig. 5A). On days 4 and 5, no significant differences in the F_v/F_m were observed, probably due to high density of the *Nostoc* culture (Fig. 5B). The relationship between F_v/F_m (PAM 2100) and F_v/F_m (Water PAM) had a linear correlation with an $R^2 = 0.668$ (Fig. 5C). The increase of F_v/F_m through the culture period can be interpreted as an improvement in the physiological status of the dense culture. Schuurmans et al. [34] demonstrated that the PAM technique inherently underestimates the photosynthetic efficiency of cyanobacteria by rendering a high F_o and a low F_m , specifically after the commonly practiced dark pre-incubation before a yield measurement. The methods applied in this study to determine, *i.e.*, dark incubation and application of DCMU or the application of darkness and Red/Far-red illumination have improved the determination of F_v/F_m by reducing the interference of elevated light induced state transitions described in cyanobacteria [34].

Thus, the reduction of absorption of red light by biliproteins can explain that *Nostoc* presents the increases F_v/F_m through the culture. It has been shown that the mutant cyanobacterium *Synechocystis* sp. (PCC 6803) with low level of biliproteins was able to present similar values of F_v/F_m to than of the green microalgae *Chlorella sorokiniana* (211-8K) and much higher than that of wild type *Synechocystis* sp. (PCC 6803) [34].

Maximal electron transport rate (ETR_{max}) increased significantly at day 5 (Fig. 6A, Table S1). Regarding the diurnal cycle, the pooled ETR_{max} showed significantly lower values in the morning (08:00 and 11:00 h) than in those in the afternoon (14:00 and 17:00 h) (Fig. 6B, Table S1). The photosynthetic efficiency (α_{ETR}) estimated from RLC increased almost four times through the experimental time, from values of about 1.1×10^{-4} in the first day to 3.9×10^{-3} after 5 days (Fig. 6C, Table S1), whereas the α_{ETR} showed no hourly variations in pooled α_{ETR} data were observed (Fig. 6D, Table S1). In the culture of *Nostoc*, the *in-situ* Y(II) values were higher than that of the *in-vivo* measurements by ~ 0.2 , with an increase to around ~ 0.25 – 0.3 on days, where data followed a trend with increased PAR irradiance. In this context, it has been demonstrated that the microalga *Chlorella fusca* showed during the first week of cultivation (days 2 and 6), lower $\Delta F'/F_m'$ (about ~ 0.15), and it is thought to be a result of too much irradiance tolerant the culture [22].

The F_v/F_m was higher on day 2 when the solar irradiance was high, suggesting no photoinhibition in the cultivation trial on this day, with a similar trend on days 4 and 5 (Fig. 5). ETR_{max} estimated from the rapid light curves (RLC) measurement *off situ*, was higher by $3.5 \mu\text{mol e}^- \text{m}^{-2} \text{s}^{-1}$ (Fig. 6), on day 5 in the late afternoon, when the cell density was higher and values of the rETR around of the $50 \mu\text{mol e}^- \text{m}^{-2} \text{s}^{-1}$. This

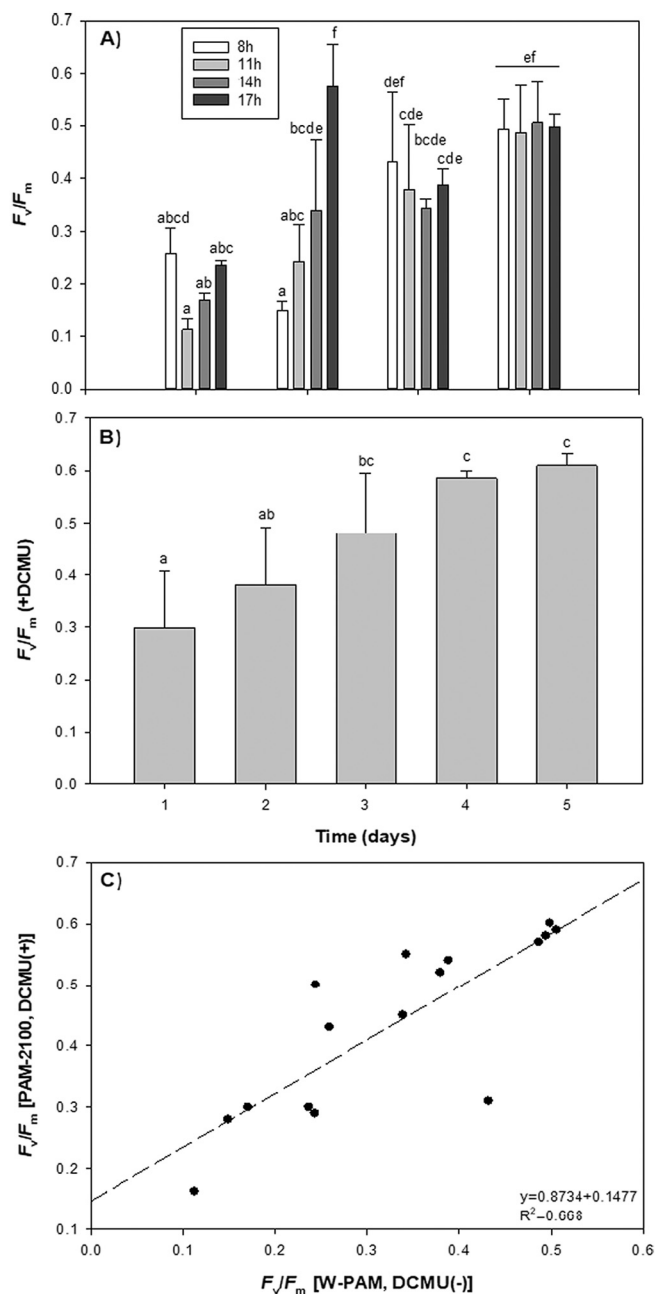


Fig. 5. Average of maximal quantum yield (F_v/F_m) determined at 08:00 h, 11:00 h, 14:00 h and 17:00 h by two methods, A) with addition of DCMU to the measuring chamber (black columns) B) with a light/dark treatment (FR + dark + R + FR) without DCMU (white histograms) and C) correlation between both methods respect to PAM 2100 and Water PAM fluorimeters equipment.

suggests higher photoacclimation in the culture trial and demonstrated the high photosynthetic efficiency at the same time. Similar results were found in *C. fusca* with $rETR_{in situ}$ values around the $50 \mu\text{mol e}^- \text{m}^{-2} \text{s}^{-1}$ [22].

The quantum-yield variables show the partitioning of absorbed excitation energy in PSII, expressed among the three complementary quantum yields: Y(II), Y(NO) and Y(NPQ) [51] which were all recorded at the last step of the RLC at $1220 \mu\text{mol photons m}^{-2} \text{s}^{-1}$ (Fig. 7). Yield loss determined as Y(NO) was the dominant component in the end of the first day of culture and the beginning of the second day. At the end of day 2 of the trial, the effective quantum yield Y(II) became the dominant component (photoacclimation), and the protective heat loss Y(NPQ) also

appeared with low values, at 11:00 and 14:00 h (Fig. 7). However, the Y (NPQ) almost disappeared in the following days. On day 3, the energy transfer through the electron chain was less than 30%, whereas the yield loss or energy dissipation was about 70%, mainly through Y(NO). On the last two days of the trial, the energy transferred through the electron transport chain increased up to 40–50% and only slight diel variations were observed. The contribution of non-photoregulated dissipation Y (NO) in the yield losses was higher during the first three days compared to the two final days, but it remains higher than of Y(NPQ) during the entire experimental period. The Y(NO) represents a loss of potential energy by the system which probably involves several factors of thermodynamic components as waste heat and losses via the Xanthophyll cycle of photosynthesis in some phototrophs [74]. Indeed, the high values of Y(NO) reflect less capacity for protection against damage by excess light compared to high Y(NPQ) values related to xanthophyll cycle system [74].

3.2. Estimation of oxygen evolution

The rate of dissolved oxygen (DO) production in the culture evolution showed a strong diel pattern with maximal values around midday (Fig. 8A). Despite the different daily irradiances, the oxygen production rate per unit area increased throughout the experimental period concurrently with an increase in biomass and Chl concentration (Fig. 8). The range of oxygen production normalized to both area ($\text{g O}_2 \text{m}^{-2} \text{h}^{-1}$) and Chl content ($\mu\text{mol O}_2 \text{mg Chl}^{-1} \text{h}^{-1}$) ranged from 0 to $2.5 \text{g O}_2 \text{m}^{-2} \text{h}^{-1}$ (Fig. 8A) and from 142 to $937 \mu\text{mol O}_2 \text{mg Chl}^{-1} \text{h}^{-1}$ (Fig. 8B), respectively. The results obtained for both equations were similar and thus validating the use of these models to assess DO production rate in the TL-RWP. The rate of oxygen production per Chl unit was maximal on day 3 showing the maximal values around midday. Maximal dissolved oxygen (DO) concentration in the culture was measured at midday and ranged from 116% saturation (day 1) to 272% saturation (day 5). The culture was initially forming large flakes, then after few days of good saturation, changed color from blue green to dark green, and formed small particles that formed homogenous suspension (Fig. 1B).

The estimate of oxygen evolution in the culture is essential for robust monitoring of photosynthetic activity under real conditions. Since the TL-RWP is a hybrid system which combines features of raceways and thin-layer cascades, two models of oxygen production were applied and compared: the model for thin-layer cascades developed by [50] and the model developed by [51] for raceway ponds. The former model considers velocity and mass transfer properties, and in the case of the latter one, the contribution of each section is considered for the mass transfer capacity of the entire unit. The results obtained from both equations were similar thus validating the use of these models to assess DO production rate in the TL-RWP. The increase in O_2 production per Chl from day 1 to day 3 can be explained by the photoacclimation of *Nostoc* to the outdoor conditions. The high photoacclimation capacity of *Nostoc* led to an increase in the photosynthetic activity which was supported by the increase in F_v/F_m , α_{ETR} , Chl content, and the decrease of phycocyanin content throughout the trial. During days 4 and 5, the O_2 production per Chl unit decreased, probably due to a lower light availability inside the culture by self-shading at a higher cell density, but the overall production per area unit did not decrease. The increase in O_2 production per unit area throughout the trial can be explained by the increase in biomass concentration, combined with photoacclimation. Nevertheless, the measured RO_2 values were lower than the range ($2\text{--}10 \text{g O}_2 \text{m}^{-2} \text{h}^{-1}$) reported by several authors for green microalgae with higher biomass concentrations [75,76,52]; however, green algae grow twice as fast as cyanobacteria under similar conditions [77]. The increase of DO concentration through the culture did not show any photoinhibition as F_v/F_m increased throughout the trial. In contrast, the increase of DO accumulation in outdoor thin layer cascades produce a decrease in the quantum yield of PSII and dynamic photoinhibition in *Chlorella vulgaris* R-117 [78]. The values of $\mu\text{mol electrons}/\mu\text{mol O}_2$ ratio was higher than

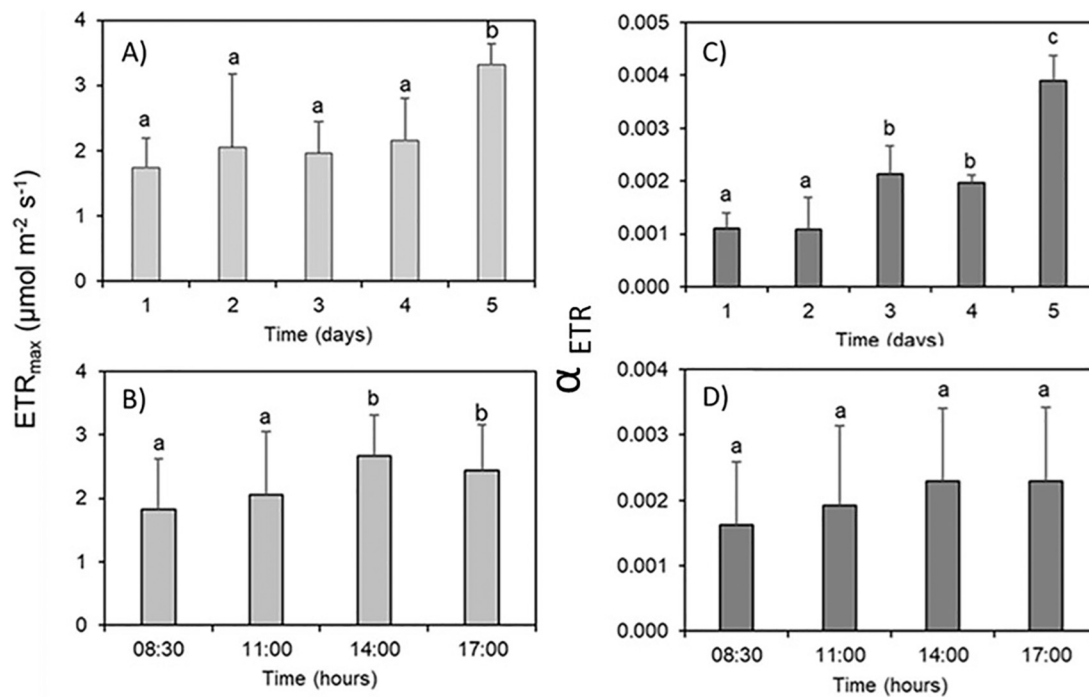


Fig. 6. Photosynthetic variables obtained from the Rapid light curves of fluorescence (ETR vs Irradiance) of *Nostoc calcicola* samples from the cultivation unit determined by the Water PAM fluorimeter; A) Pooled data of the maximal electron transport rate (ETR_{max}) according to significant differences in time (days of the trial), B) Pooled data of the maximal electron transport rate (ETR_{max}) according to significant differences in time (hours; 08:00 h, 11:00 h, 14:00 h, and 17:00 h), C) Pooled data of the Photosynthetic efficiency (α_{ETR}) according to significant differences in time (days of the trial), and D) Pooled data of the Photosynthetic efficiency (α_{ETR}) according to significant differences in time (hours; 08:00 h, 11:00 h, 14:00 h, and 17:00 h). Results are expressed in a percentage as means \pm standard deviation ($n = 3$).

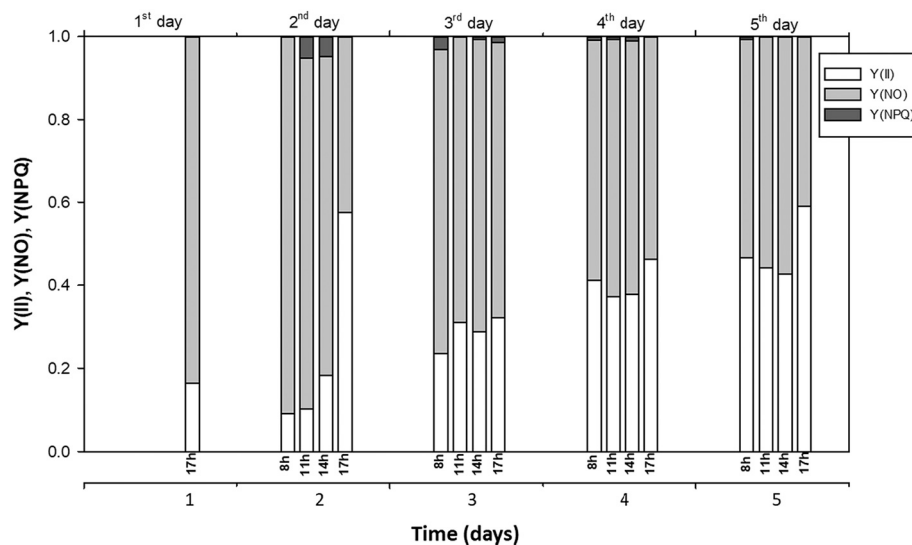


Fig. 7. Effective quantum yield $Y(II)$, Yield Loss: $Y(NO)$ and $Y(NPQ)$ measurements throughout the day, at different time (08:00, 11:00, 14:00 and 17:00 h). The data were calculated from the fluorescence parameters in rapid light curves at exposure of $1500 \mu\text{mol m}^{-2} \text{s}^{-1}$.

predicted, suggesting the probable involvement of electron and oxygen consuming processes such as photorespiration and the Mehler reaction [78]. These processes probably function as photoprotective mechanisms, since no photodamage was observed in the *Chlorella* R-117 cultures [78].

3.3. Bio-active compounds

Total internal carbon content generally showed a significant increase

during the experiment, especially at 17:00 h (Table 1). The carbon content was generally higher in the samples taken in the morning as compared to that in the afternoon (Table 1). The ratio of total carbon to total nitrogen content (C:N) ranged between 4.33 (initial time) up to 5.76 found during the third day when the sample was taken at 17:00 h. Generally, the C:N ratio showed an increasing trend from the start to the end of the trial. The nutritional state, seen in the quantity of internal carbon and ratio of C:N content, was higher during days 4 and 5 of the trial, respectively. This suggests that nitrogen incorporation into the

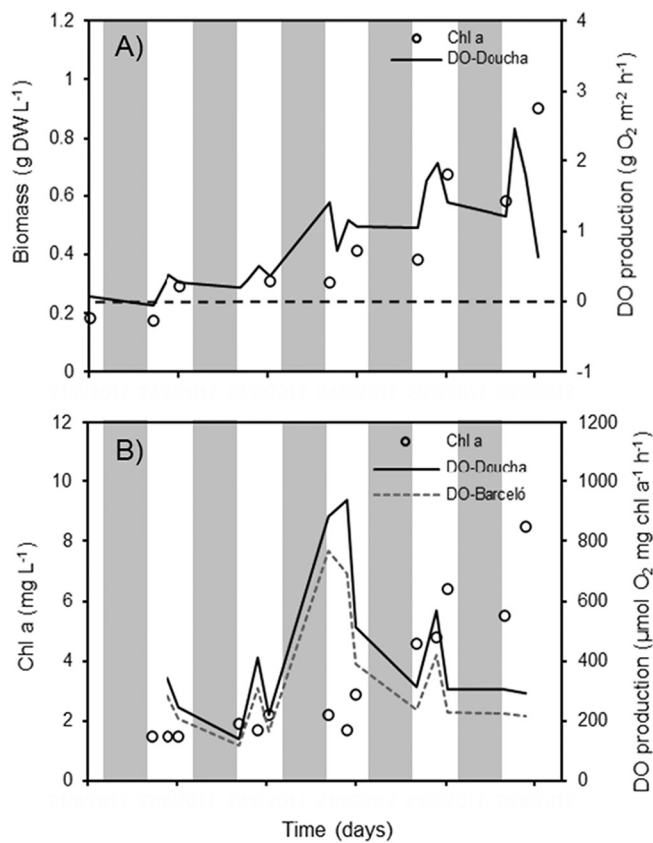


Fig. 8. A) Concentration of chlorophyll *a* in mg L⁻¹ and the rate of dissolved oxygen (DO) expressed in g O₂ m⁻² h⁻¹ as RO₂ vs irradiance and versus μmol O₂ in the thin-layer raceway pond during the growth of *Nostoc calcicola* and B) Validation of the models to assess DO production rate in the TL-RWP according to Doucha and Lívanský [85] and Barceló-Villalobos et al. [53].

Table 1

Total internal Carbon content (mg g⁻¹ DW) and the ratio of total internal carbon and total internal nitrogen quantified in the cyanobacterium *Nostoc calcicola* during the 5-day cultivation trial in a thin-layer raceway pond. Results are expressed as means ± standard deviation (n = 3). Values with the same symbol did not differ significantly from each other (p > 0.05).

Day	Carbon		Ratio Carbon: Nitrogen	
	08:00 h	17:00 h	08:00 h	17:00 h
Day 0				
Day 1	43.51 ± 0.08 ^b	42.02 ± 0.73 ^d	4.49 ± 0.02 ^B	4.70 ± 0.03 ^A
Day 2	44.11 ± 0.11 ^{ab}	44.28 ± 0.82 ^{ab}	4.67 ± 0.01 ^A	5.35 ± 0.10 ^E
Day 3	46.35 ± 0.11 ^c	44.42 ± 0.15 ^{ab}	5.06 ± 0.01 ^C	5.76 ± 0.08 ^G
Day 4	46.21 ± 0.27 ^c	45.05 ± 0.01 ^a	4.67 ± 0.01 ^A	5.62 ± 0.02 ^F
Day 5	44.96 ± 0.12 ^a	47.76 ± 0.09 ^e	4.50 ± 0.02 ^A	5.22 ± 0.08 ^D

biomass was slower than that of carbon. Besides, the values of protein, starch and lipid content were found higher at the end of the trial, with the figures around 43.8, 27.9 and 7.2%, respectively. The aquatic cyanobacterium *N. verrucosum* produces massive extracellular polysaccharides and accumulates trehalose in response to desiccation, unlike the anhydrobiotic cyanobacterium *N. commune* is not sensitive to desiccation [79]. Carbohydrates of *Nostoc commune* present antioxidant capacity [80].

Chl content in the biomass generally increased through the experimental period, i.e., from 4 to about 9–12 mg DW g⁻¹ (Fig. 9A, Table S1).

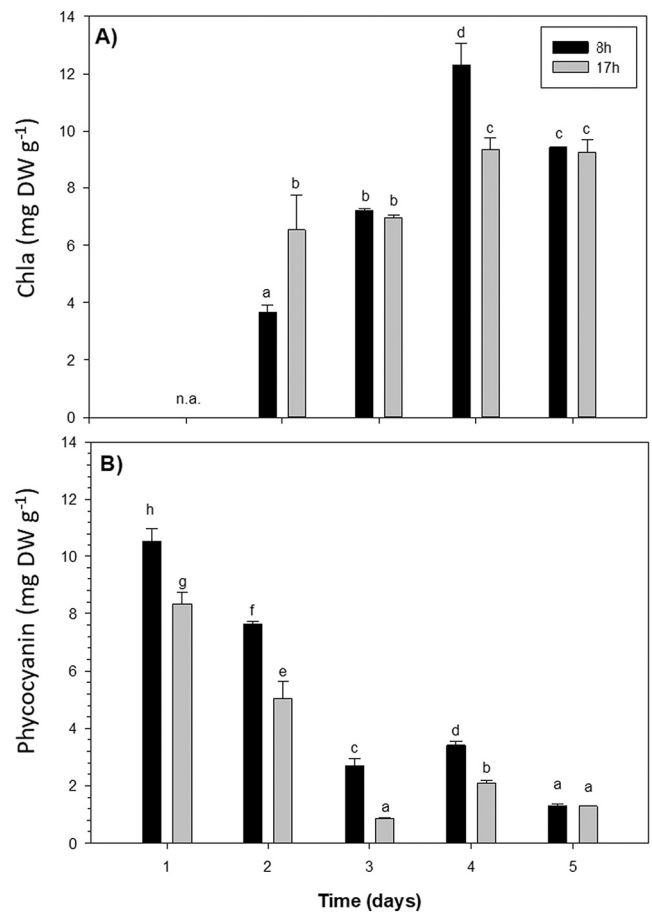


Fig. 9. A) Content of chlorophyll *a* and B) Phycocyanin (PC) expressed in *Nostoc* (g DW g⁻¹) calculated through the experimental time. Results are expressed in a percentage as means ± standard deviation (n = 3).

Table 2

The content (% DW) of total proteins, starch and lipids quantified in the culture of cyanobacterium *Nostoc calcicola* throughout 5 days of cultivation in a thin-layer raceway pond. Results are expressed in a percentage as means ± standard deviation (n = 3). Values with the same symbol did not differ significantly from each other (p > 0.05).

Day	Proteins		Starch		Lipids	
	08:00 h	17:00 h	08:00 h	17:00 h	08:00 h	17:00 h
Day 0						
Day 1	46.31 ± 0.16 ^a	42.71 ± 0.47 ^a	19.28 ± 7.40 ^b	19.28 ± 26.18 ± 2.94	1.91 ± 0.04 ^A	1.84 ± 0.17 ^A
Day 2	45.16 ± 0.10 ^b	39.55 ± 0.30 ^b	27.56 ± 6.60 ^{ab}	28.97 ± 3.34 ^{ab}	3.28 ± 0.72 ^A	1.78 ± 0.69 ^A
Day 3	43.81 ± 0.08 ^b	36.88 ± 0.39 ^d	27.28 ± 6.30 ^{ab}	32.92 ± 7.34 ^a	2.67 ± 0.03 ^A	1.98 ± 0.23 ^A
Day 4	47.3 ± 0.20 ^f	38.33 ± 0.12 ^a	23.39 ± 2.80 ^{ab}	33.95 ± 6.66 ^a	5.22 ± 1.74 ^B	3.3 ± 0.78 ^A
Day 5	47.71 ± 0.30 ^e	43.77 ± 0.54 ^c	17.64 ± 6.50 ^{ab}	27.94 ± 3.33 ^{ab}	2.27 ± 0.71 ^A	7.2 ± 0.51 ^C

The morning-afternoon variation was inconsistent, going one way or the other on each day (Fig. 9A). However, Phycocyanin (PC) content dropped from about 12 mg DW g⁻¹ to less than 2 mg DW g⁻¹ with the progression of the experiment and was significantly higher (Table S1) in the morning samples (08:00 h) as compared to these taken in the afternoon (17:00 h), except for the last day, where the morning and

Table 3

The content of phenolic compounds (mg DW g^{-1}), antioxidant activity through the ABTS (2,2'-azino-bis (3-ethylbenzothiazoline-6-sulfonic acid)) method (TEAC: Trolox Equivalent Antioxidant Capacity in g DW^{-1}) and the content of mycosporine-like amino acid (mg DW g^{-1}) quantified in *Nostoc calcicola* throughout the 5-day trial using a thin-layer raceway pond. Results are expressed in a percentage as means \pm standard deviation ($n = 3$). Values with the same symbol did not differ significantly from each other ($p > 0.05$).

Days	Phenolic compounds		ABTS method		MAAs			
	08:00	17:00	08:00	17:00	UVAC1	UVAC2	UVAC3	UVAC4
Initial time		4.50 \pm 0.38		106.85 \pm 2.16				
First day	3.77 \pm 0.36 ^a	2.81 \pm 0.47 ^c	89.92 \pm 1.74 ^{d*}	101.70 \pm 2.34 ^{f*}	38.64 \pm 0.66 ^b	24.62 \pm 1.67 ^b	34.63 \pm 2.21 ^{ab}	0.00 \pm 0.00
Second day	3.62 \pm 0.10 ^a	3.49 \pm 0.13 ^a	129.43 \pm 3.06 ^{g*}	122.58 \pm 2.60 ^{f*}	37.15 \pm 0.40 ^b	25.89 \pm 0.44 ^b	36.96 \pm 0.28 ^b	0.00 \pm 0.00
Third day	3.55 \pm 0.14 ^a	4.41 \pm 0.24 ^d	149.55 \pm 3.91 ^{b*}	116.02 \pm 2.38 ^{e*}	35.22 \pm 2.38 ^{ab}	19.89 \pm 2.17 ^a	32.07 \pm 2.02 ^a	12.83 \pm 2.20 ^a
Fourth day	6.46 \pm 0.30 ^e	5.57 \pm 0.54 ^b	146.28 \pm 3.39 ^{b*}	133.93 \pm 2.40 ^{h*}	33.55 \pm 2.14 ^a	18.90 \pm 2.08 ^a	30.82 \pm 2.38 ^a	16.74 \pm 3.00 ^b
Fifth day	5.69 \pm 0.31 ^b	5.90 \pm 0.17 ^b	101.94 \pm 2.26 ^{a*}	48.02 \pm 0.26 ^{c*}	38.18 \pm 1.52 ^b	19.84 \pm 0.22 ^a	33.28 \pm 1.19 ^{ab}	21.04 \pm 2.04 ^c

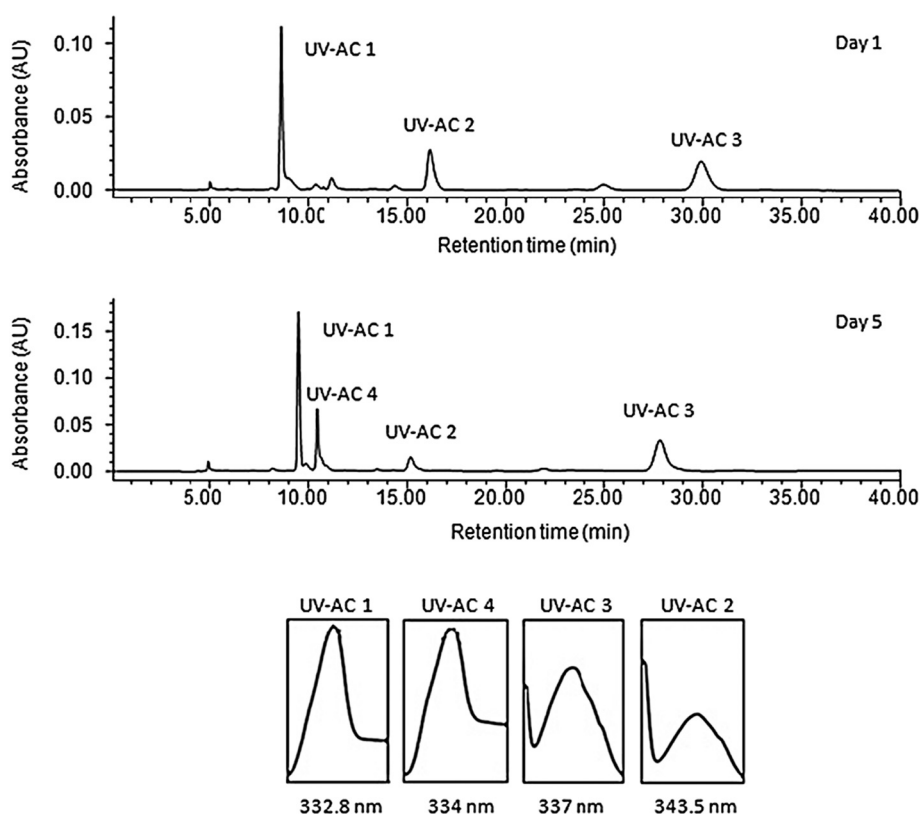


Fig. 10. HPLC chromatograms of UV-absorbing compounds extracted from *Nostoc calcicola* on the first and last day, and absorption spectra of the selected four peaks from the chromatograms. Only the first peak (UV-AC1) was identified as the mycosporine-like amino acid Shinorine, with a maximal absorption at 332.8 nm.

afternoon value did not differ significantly from each other (Fig. 9B, Table S1). The Chl and Phycocyanin responded inversely throughout the experimental period. The increase in Chl content can be related to increase of antioxidant capacity associated with this pigment as it has been reported by [81]. Phycobilin can also have antioxidant activity and it certainly exhibits radical scavenging activity in dark environments, though it also generates hydroxyl radicals in light environments. There was significant, but inconsistent variability in the content of total protein and total lipid between days (Table 2). The carbohydrate content was mostly higher in the afternoon at 17:00 h samples as compared to those taken in the morning at 08:00 h. The carbohydrate content consistently increased from the initial value of $19.28 \pm 2.84 \text{ mg DW g}^{-1}$ to $33.95 \pm 6.6 \text{ mg DW g}^{-1}$ on day 4 of the trial, but dropped on day 5 (Table 2). The daily differences between morning and afternoon values were consistent, with the protein and lipid content being generally higher in the morning than in the afternoon except for the last day. The

major fatty acid in the *Nostoc* culture was palmitic acid with around 36–39%, followed by linoleic acid with 24–28%, in combination, both fatty acids represented more than of the 50% of total fatty acid content (Table S2). Thus, after day - 5 of cultivation, the content of palmitic, oleic and linoleic acids was higher, that stearic, and α -linoleic acids (Table S2).

Polyphenol content increased throughout the experiment from 3 to 6.5 mg DW g^{-1} (Table 3). The morning-afternoon variations in polyphenol content were significant but inconsistent from day to day (Table 3). The antioxidant activity increased from the start of the trial to the end, i.e., 90–100 to $150 \mu\text{mol TEAC}$ (Trolox Equivalent Antioxidant Capacity) g DW^{-1} . During the last day of cultivation, the antioxidant activity drastically decreased, mainly in the afternoon samples (Table 3). In general, the morning antioxidant activity was higher than that in the afternoons. A positive correlation between polyphenol content and antioxidant activity and phenolic compounds accumulated

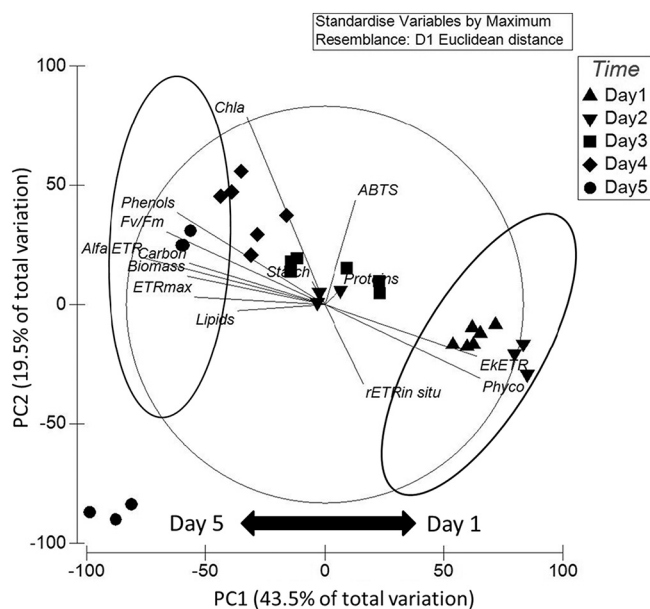


Fig. 11. Principal components analyses in relation to time (from day 1 to day 5). Vectors overlay (Spearman rank correlation) indicates the relationship between the PCO axes and the ecophysiological (F_v/F_m , ETR_{max} , α_{ETR} , Ek_{ETR} , $rETR_{in situ}$), and biochemical (Phenols, ABTS, Chl *a*, Phycocyanin, Carbon, Proteins, Starch and Lipids), variables throughout time during the cultivation trial.

especially in the later days of the experiment (Table S3). In *Nostoc commune*, the antioxidant capacity was also related to the content of polyphenols [16].

The composition of the mycosporine-like amino acids (MAAs) was evaluated by liquid chromatography detecting three peaks of UV-absorbing compounds (Table 3 and Fig. 10). The first peak (UV-AC1) with the maximal absorption at 332.8 nm was dominant; it corresponds to the MAA shinorine and the content decreased throughout the trial (Table 3 and Fig. 10). Other two peaks were determined at higher retention time and could not be related to any known MAAs. They were designated as UV-AC2 and UV-AC3 with the absorption peaks at 343.5 and 337 nm. These two UV absorbing compounds decreased also through the experimental time. Another peak, designated as UV-AC4 with the 334-nm absorption peak (Fig. 10), was detected on day 3, where content was increasing and reached about two times higher value during the last day of cultivation. The presence of the MAAs Porphyrin-334 and Shinorine and an unknown UV absorbing compound was also reported in *Nostoc* sp. [15].

MAAs absorb UV-A radiation and can dissipate the absorbed light energy as heat without reactive radical species (ROS) production [82]. Several MAAs in cyanobacteria present high antioxidant capacity [16]. Several authors reported that antioxidant scavenging activity of mycosporine-glycine, as determined by ABTS, is far greater than that of Porphyrin-334, Shinorine, Palythine, Palythanol and Asterina-330 [83,84]. On the contrary, Asterina-330, Porphyrin-334 and Shinorine showed higher protection against lipid peroxidation than that of mycosporine-glycine [84]. In our study, high temperature fluctuations were produced by solar irradiance, while UV radiation was blocked from entering the greenhouse. It was observed that mycosporine-glycine was under constitutive control, while Porphyrin-334 and shinorine were induced by UV-B radiation, indicating the involvement of UV-regulated enzymes in the biotransformation of MAAs [84]. Despite this, UV-absorbing compounds include the identified MAA, shinorine, whose content increased throughout the experimental period. The accumulation of MAAs is controlled not only by UV radiation, but also by nitrate

availability. Thus, the culture medium enriched by nitrogen can positively influence in the accumulation of MAAs despite the absence of UV radiation within of greenhouse.

3.4. Pearson correlations and principal coordinates analysis

The Pearson correlation showed a positive correlation between Ek_{ETR} , Yield (II), and α_{ETR} throughout all experimental period (Table S3). Furthermore, a positive correlation was found between Ek_{ETR} and Yield (II), and between ETR_{max} and Proteins. Y(NO), Y(NPQ) and PC were positively correlated (Table S3). Finally, a positive correlation was found between Chl and phenols, starch, and C:N, $rETR_{in situ}$, and lipids (Table S3).

The two first dimensions of the Principal Coordinates Analysis (PCO diagram) based on both photosynthetic and biochemical variables represented 63% of total data set variation (Fig. 11). These analyses with *Nostoc* culture, shows a positive correlation of the first axis (43.5% of total variation) with Ek_{ETR} , Phycocyanin, $rETR_{in situ}$, proteins being highest in the samples from the initial time of the experimental period (Fig. 11). On the contrary, phenols, F_v/F_m , Chl, α_{ETR} , carbon, biomass, ETR_{max} , lipids were the highest in the samples collected at the end of the experimental period (day 5) being positively correlated with the second dimension (19.5% of the total variation). The small angles between the arrows indicate a high positive correlation between the variables (Fig. 11). The combination of these variables allowed separating the time of the photoacclimation for this studied species, revealing that considering the physiological and biochemical variables measured in *Nostoc*, exhibited species-specific responses to increase along the experimental time.

4. Conclusions

We aimed to correlate photosynthetic activity, biochemical characteristics and biomass productivity of a microalgae culture grown in a high rate TL-RWP. The optimal availability of light energy in the TL-RWP has beneficial effects on growth and accumulation of bio-active compounds. The simultaneous assessment of multiple variables was used to monitor changes in the culture of *Nostoc calcicola* (MACC-612) during the 5-day trial. In this study, it was demonstrated that the TL-RWP is suitable for culturing fast-growing filamentous cyanobacteria *Nostoc calcicola*. The photophysiological and biochemical responses were correlated with outdoor conditions during the trial. This corresponded with the high photoacclimation capacity of this cyanobacteria. The biomass, F_v/F_m , ETR, photosynthetic efficiency, Chl and carbon content increased along the trial period. This biochemical composition, mainly the high carbon content and the accumulation of antioxidant substances as Chl, polyphenols and MAAs in *this strain*, suggesting of biotechnological potential of the strain such as production of cosmetics when outdoors in thin-layer raceway ponds.

CRediT authorship contribution statement

Paula S.M. Celis-Plá, Investigation, conceptualization, formal analysis, writing-original draft & editing. Jiří Masojídek, Giuseppe Torzillo, Félix López Figueroa, Amir Neori, Tomás Agustín Rearte, Karolína Ranglová and Peter Ralph, Investigation, conceptualization, writing review & editing. José Bonomi-Barufi, Félix Álvarez-Gómez, Jaqueline Carmo da Silva, Roberto Abdala, Cintia Gómez, Martín Caporgno, Ana Margarita Silva Benavides, Thaís Fávero Massocato, Richard Atzmüller, Julia Vega and Patricia Chávez, Investigation & data analysis.

Declaration of competing interest

The authors declare that they have no known competing financial interests or personal relationships that could have appeared to influence

the work reported in this paper.

Acknowledgments

The authors thank Ms. Soňa Pekarová, Mr. Jan Pilný, Mr. Michal Bureš and Mr. Petr Novotný for technical assistance and Dr. Richard Lhotský for experiment management. The authors thank to the local organizers of Algatex Center of the Institute of Microbiology (Czech Academic of Sciences) the organization of GAP10 workshop “Aquatic productivity - in the Omics Era”, held in Třeboň (Czech Republic) between 19 and 30 August 2017.

Funding

This work was supported by the EU program Horizon 2020 (project SABANA, grant no. 727874) and in part by the Program INTERREG V-A Austria – Czech Republic, project ATCZ221 Algae 4 Fish. PSMCP was supported by the Santander scholarship to young research 2017 and project FONDECYT N° 11180197. FLF thanks Junta de Andalucía for financial support of the research group “Photobiology and biotechnology of aquatic organisms” (FYBOA-RNM295). TAR was supported by the Universidad de Buenos Aires, Argentina. AN thanks BARD Research Grant Award No. US – 4599-13R (The United States – Israel Binational Agricultural Research and Development Fund) and additional funds from the Israeli Ministry for Science and Technology and the Dead Sea-Arava Science Center (DSASC) to AN.

Dedication

This special issue of Algal Research is dedicated to Prof. Jacco Kromkamp, regular participant and organizer of GAP workshops, who unluckily passed away in October 2020.

Appendix A. Supplementary data

Supplementary data to this article can be found online at <https://doi.org/10.1016/j.algal.2021.102421>.

References

- [1] A. Willis, J.N. Woodhouse, Defining cyanobacterial species: diversity and description through genomics, *Crit. Rev. Plant Sci.* (2020) 1–24. <https://doi.org/10.1080/07352689.2020.1763541>.
- [2] D. Wright, T. Prickett, R.F. Helm, M. Potts, Form species *Nostoc commune* (cyanobacteria), *Int. J. Syst. Evol. Microb.* 51 (5) (2001) 1839–1852. <https://doi.org/10.1099/00207713-51-5-1839>.
- [3] F.M. Morsy, S. Kuzuha, Y. Takani, T. Sakamoto, Novel thermostable glycosidases in the extracellular matrix of the terrestrial cyanobacterium *Nostoc commune*, *J. Gen. Appl. Microbiol.* 54 (5) (2008) 243–252. <https://doi.org/10.2323/jgam.54.243>.
- [4] K. Sand-Jensen, Ecophysiology of gelatinous *Nostoc* colonies: unprecedented slow growth and survival in resource-poor and harsh environments, *Ann. Bot.* 114 (1) (2014) 17–33. <https://doi.org/10.1093/aob/mcu085>.
- [5] S. Mazard, A. Penesyan, M. Ostrowski, I.T. Paulsen, S.T. Egan, Microbes with a big impact: the role of cyanobacteria and their metabolites in shaping our future, *Mar. Drugs* 14 (2016) 97. <https://doi.org/10.3390/md14050097>.
- [6] N.K. Lee, H.-M. Ok, H.-S. Kim, C.Y. Ahn, Higher production of C-phycoerythrin by nitrogen-free (diazotrophic) cultivation of *Nostoc* sp. NK and simplified extraction by dark-cold shock, *Ciorenour. Technol.* 227 (2017) 164–170. <https://doi.org/10.1016/j.biortech.2016.12.053>.
- [7] M.S. Hashtroudi, A. Ghassempour, H. Riahi, Z. Shariatmadari, M. Khanjir, Endogenous auxins in plant growth-promoting Cyanobacteria—*Anabaena vaginicola* and *Nostoc calcicola*, *J. Appl. Phycol.* 25 (2) (2013) 379–386. <https://doi.org/10.1007/s10811-012-9872-7>.
- [8] V.E. Niveshika, A.K. Mishra, A.K. Singh, V.K. Singh, Structural elucidation and molecular docking of a novel antibiotic compound from Cyanobacterium *Nostoc* sp. MGL001, *Front. Microbiol.* 7 (2016) 1899. <https://doi.org/10.3389/fmicb.2016.01899>.
- [9] S. Ramachandran, T. Coradin, P.K. Jain, S.K. Verma, *Nostoc calcicola* immobilized in silica-coated calcium alginate and silica gel for applications in heavy metal biosorption, *Silicon* 1 (4) (2009) 215–223. <https://doi.org/10.1007/s12633-009-9032-0>.
- [10] J. Morone, A. Alfeus, V. Vasconcelos, R. Martins, Revealing the potential of cyanobacteria in cosmetics and cosmeceuticals—a new bioactive approach, *Algal Res.* 41 (2019), 101541. <https://doi.org/10.1016/j.algal.2019.101541>.
- [11] M. Krause, A. Klit, M. Bomberg-Jensen, T. Soeborg, H. Frederiksen, M. Schlumpf, W. Lichtensteiger, N.E. Skakkebaek, K.T. Drzewiecki, Sunscreens: are they beneficial for health? An overview of endocrine disrupting properties of UV-filters, *Int. J. Androl.* 35 (2012) 424–436. <https://doi.org/10.1111/j.1365-2605.2012.01280.x>.
- [12] V. Sarveiya, S. Risk, H.A.E. Benson, Liquid chromatographic assay for common, sunscreen agents: application to in vivo assessment of skin penetration and systemic absorption in human volunteers, *J. Chromatogr. B* 8 (2004) 225–231. <https://doi.org/10.1016/j.jchromb.2003.12.022>.
- [13] J. Kockler, M. Oelgemoller, S. Robertson, D. Glass, Photostability of sunscreens, *J. Photochem. Photobiol. C* 13 (2012) 91–110. <https://doi.org/10.1016/j.jphotochemrev.2011.12.001>.
- [14] D. Sánchez-Quiles, A. Tovar-Sánchez, Sunscreens as a source of hydrogen peroxide production in coastal waters, *Environ. Sci. Technol.* 48 (2014) 9037–9042. <https://doi.org/10.1021/es5020696>.
- [15] R.P. Richa, Sinha, Biochemical characterization of suncreening mycosporine-like amino acids from two *Nostoc* species inhabiting diverse habitats, *Protoplasma* 252 (2015) 199–208. <https://doi.org/10.1007/s00709-014-0674-4>.
- [16] J. Vega, J. Bonomi-Barufi, J.L. Gómez-Pinchetti, F.L. Figueroa, Cyanobacteria and red macroalgae as potential source of antioxidants and UV radiation absorbing compounds for cosmeceutical applications, *Mar Drugs* 18 (2020) 659. <https://doi.org/10.3390/md18120659>.
- [17] P. Derikvand, C.A. Llewellyn, S. Purton, Cyanobacterial metabolites as a source of sunscreens and moisturizers: a comparison with current synthetic compounds, *Eur. J. Phycol.* 52 (2016) 43–56. <https://doi.org/10.1080/09670262.2016.1214882>.
- [18] P.P. Han, Y. Sun, X.Y. Wu, Y.J. Yuan, Y.J. Dai, S.R. Jia, Emulsifying, flocculating, and physicochemical properties of exopolysaccharide produced by cyanobacterium *Nostoc flagelliforme*, *Appl. Biochem. Biotechnol.* 172 (1) (2014) 36–49. <https://doi.org/10.1007/s12010-013-0505-7>.
- [19] T. Grival'ský, K. Ráňglová, J.A. da Câmara Manoel, G.E. Lakatos, R. Lhotský, J. Masojídek, Development of thin-layer cascades for microalgae cultivation: milestones (review), *Folia Microbiol. (Praha)* 64 (5) (2019) 603–614. <https://doi.org/10.1007/s12223-019-00739-7>.
- [20] J. Masojídek, M. Sergejevo'ová, J.R. Malapascua, J. Kopecký, Thin-layer systems for mass cultivation of microalgae: flat panels and sloping cascades, in: R. Bajpai, A. Prokop, M. Zappi (Eds.), *Algal Biorefinery vol. 2*, Springer International Publishing, Switzerland, 2015, pp. 237–262. https://doi.org/10.1007/978-3-319-20200-6_7.
- [21] J. Masojídek, J. Kopecký, L. Giannelli, G. Torzillo, Productivity correlated to photobiochemical performance of *Chlorella* mass cultures grown outdoors in thin-layer cascades, *J. Ind. Microbiol. Biotechnol.* 38 (2011) 307–317. <https://doi.org/10.1007/s10295-010-0774-x>.
- [22] C.G. Jerez, J.R. Malapascua, M. Sergejevo'ová, J. Masojídek, F.L. Figueroa, *Chlorella fusca* (Chlorophyta) grown in thin-layer cascades: estimation of biomass productivity by in-vivo chlorophyll a fluorescence monitoring, *Algal Res.* 17 (2016) 21–30. <https://doi.org/10.1016/j.algal.2016.04.010>.
- [23] J.U. Grobelaar, Upper limits of photosynthetic productivity and problems of scaling, *J. Appl. Phycol.* 21 (2009) 519–522. <https://doi.org/10.1007/s10811-008-9372-y>.
- [24] J. Masojídek, A. Vonshak, G. Torzillo, Chlorophyll fluorescence applications in microalgal mass cultures, in: D.J. Suggett, O. Prášil, M.A. Borowitzka (Eds.), *Chlorophyll a Fluorescence in Aquatic Sciences: Methods and Applications*, Springer Netherlands, Netherlands, 2010, pp. 277–292. https://doi.org/10.1007/978-90-481-9268-7_13.
- [25] J. Masojídek, G. Torzillo, M. Koblížek, G. Torzillo, Photosynthesis in microalgae, in: A. Richmond (Ed.), *Handbook of Microalgal Culture*, Blackwell Publishing Ltd, Oxford, UK, 2013, pp. 21–36. <https://doi.org/10.1002/9781118567166>.
- [26] J.C. Kromkamp, R.M. Forster, The use of variable fluorescence measurements in aquatic ecosystems: differences between multiple and single turnover measuring protocols and suggested terminology, *Eur. J. Phycol.* 38 (2003) 103–112. <https://doi.org/10.1080/0967026031000094094>.
- [27] N.R. Baker, Chlorophyll fluorescence: a probe of photosynthesis in vivo, *Annu. Rev. Plant Biol.* 59 (2008) 89–113. <https://doi.org/10.1146/annurev.arplant.59.0326.07.092759>.
- [28] I.A. Flameling, J. Kromkamp, Light dependence of quantum yields for PSII charge separation and oxygen evolution in eucaryotic algae, *Limnol. Oceanogr.* 43 (1998) 284–297. <https://doi.org/10.4319/lo.1998.43.2.0284>.
- [29] F.L. Figueroa, R.M. Conde-Álvarez, I. Gómez, Relations between electron transport rates determined by pulse amplitude modulated chlorophyll fluorescence and oxygen evolution in macroalgae under different light conditions, *Photosynth. Res.* 75 (2003) 259–275. <https://doi.org/10.1023/A:1023936313544>.
- [30] E. Lawrenz, G. Silsbe, E. Capuzzo, P. Ylostalo, R.M. Forster, S.G.H. Simis, O. Prasil, J.C. Kromkamp, A.E. Hickman, C.M. Moore, M.-H. Forget, R.J. Geider, D. J. Suggett, Predicting the electron requirement for carbon fixation in seas and oceans, *PLoS One* 8 (3) (2013), e58137. <https://doi.org/10.1371/journal.pon.e0058137>.
- [31] U. Schreiber, U. Schliwa, W. Bilger, Continuous recording of photochemical and non-photochemical chlorophyll fluorescence quenching with a new type of modulation fluorometer, *Photosynth. Res.* 10 (1–2) (1986) 51–62. <https://doi.org/10.1007/BF00024185>.
- [32] F.L. Figueroa, C.G. Jerez, N. Korbee, Use of in vivo chlorophyll fluorescence to estimate photosynthetic activity and biomass productivity in microalgae grown in different culture systems, *Lat. Am. J. Aquat. Res.* 41 (2013) 801–819. <https://doi.org/10.3856/vol41-issue5-fulltext-1>.
- [33] D. Campbell, V. Hurry, A.K. Clarke, P. Gustafsson, G. Oquist, Chlorophyll fluorescence analysis of cyanobacterial photosynthesis and acclimation, *Microbiol.*

- Mol. Biol. Rev. 62 (3) (1998) 667–683. <https://doi.org/10.1128/MMBR.62.3.667-683.1998>.
- [34] R.M. Schuurmans, P. van Alphen, J.M. Schuurmans, H.C.P. Matthijs, K. J. Hellingwerf, Comparison of the photosynthetic yield of cyanobacteria and green algae: different methods give different answers, *PLoS ONE* 10 (9) (2015), e0139061. <https://doi.org/10.1371/journal.pone.0139061>.
- [35] M.M. Allen, R.Y. Stanier, Growth and division of some unicellular blue-green algae, *J. Gen. Microbiol.* 51 (1968) 199–202. <https://doi.org/10.1099/00221287-51-2-199>.
- [36] K. Rangelová, G.E. Lakatos, J.A.C. Manoel, T. Grivalský, J. Masojídek, Rapid screening test to estimate temperature optima for microalgae growth using photosynthesis activity measurements, *Folia Microbiol. (Praha)* 64 (5) (2019) 615–625. <https://doi.org/10.1007/s12223-019-00738-8>.
- [37] K. Shibata, A.A. Benson, M. Calvin, The absorption spectra of suspensions of living micro-organisms, *Biochim. Biophys. Acta* 15 (1954) 461–470. [https://doi.org/10.1016/0006-3002\(54\)90002-5](https://doi.org/10.1016/0006-3002(54)90002-5).
- [38] B. Arbones, F.G. Figueiras, M. Zapata, Determination of phytoplankton absorption coefficient in natural seawater samples: evidence of a unique equation to correct the pathlength amplification on glass-fiber filters, *Mar. Ecol. Prog. Ser.* 137 (1996) 293–304. <https://doi.org/10.3354/meps137293>.
- [39] C.G. Jerez, C.B. García, A. Rearte, F.L. Figueroa, Relation between light absorption measured by the quantitative filter technique and attenuation of *Chlorella fusca* cultures of different cell densities: application to estimate the absolute electron transport rate (ETR), *J. Appl. Phycol.* 28 (2016) 1635–1648. <https://doi.org/10.1007/s10811-015-0685-3>.
- [40] P.S.M. Celis-Plá, J.M. Hall-Spencer, P.A. Horta, M. Milazzo, N. Korbee, C. E. Cornwall, F.L. Figueroa, Macroalgal responses to ocean acidification depend on nutrient and light levels, *Mar. Sci.* 2 (2015) 26. <https://doi.org/10.3389/fmars.2015.00026>.
- [41] C.G. Jerez, E. Navarro, I. Malpartida, R.M. Rico, J. Masojídek, R. Abdala, F. L. Figueroa, Hydrodynamics and photosynthesis performance of *Chlorella fusca* grown in a Thin-Layer Cascade (TLC) system, *Aquat. Biol.* 22 (2014) 111–122. <https://doi.org/10.3354/ab00603>.
- [42] P.S.M. Celis-Plá, N. Korbee, A. Gómez-Garreta, F.L. Figueroa, Seasonal photoacclimation patterns in the intertidal macroalga *Cystoseira tamariscifolia* (Ochrophyta), *Sci. Mar.* 78 (3) (2014) 377–388. <https://doi.org/10.3989/scimar.04053.05A>.
- [43] G. Johnsen, E. Sakshaug, Biooptical characteristics of PSII and PSI in 33 species (13 pigment groups) of marine phytoplankton, and the relevance for pulse amplitude-modulated and fast-repetition-rate fluorometry, *J. Phycol.* 43 (2007) 1236–1251. <https://doi.org/10.1111/j.1529-8817.2007.00422.x>.
- [44] D.J. Suggett, H.L. MacIntyre, R.J. Geider, Evaluation of biophysical and optical determinations of light absorption by photosystem II in phytoplankton, *Limnol. Oceanogr. Methods* 2 (2004) 316–332. <https://doi.org/10.4319/lom.2004.2.316>.
- [45] D. Hanelt, B. Melchersmann, C. Wiencke, W. Nultsch, Effects of high light stress on photosynthesis of polar macroalgae in relation to depth distribution, *Mar. Ecol. Prog. Ser.* 149 (1997) 255–266. <https://doi.org/10.3354/meps149255>.
- [46] P.H.C. Eilers, J.C.H. Peeters, A model for the relationship between light intensity and the rate of photosynthesis in phytoplankton, *Ecol. Model.* 42 (1988) 199–215. [https://doi.org/10.1016/0304-3800\(88\)90057-9](https://doi.org/10.1016/0304-3800(88)90057-9).
- [47] W. Bilger, U. Schreiber, M. Bock, Determination of the quantum efficiency of photosystem II and of non-photochemical quenching of chlorophyll fluorescence in the field, *Oecologia* 102 (4) (1995) 425–432. <https://doi.org/10.1007/BF00341354>.
- [48] P.S.M. Celis-Plá, Z. Bouzon, J.M. Hall-Spencer, E. Schmidt, N. Korbee, F. L. Figueroa, Seasonal biochemical and photophysiological responses in the intertidal macroalga *Cystoseira tamariscifolia* (Ochrophyta), *Mar. Environ. Res.* 115 (2016) 89–97. <https://doi.org/10.1016/j.marenvres.2015.11.014>.
- [49] D.M. Kramer, G. Johnson, O. Kírats, G.E. Edwards, New fluorescence parameters for the determination of QA redox state and excitation energy fluxes, *Photosynth. Res.* 79 (2004) 209–218 (<https://doi.org/10.1023%2FB3APRES.0000015391.99477.0d>).
- [50] L. Hendrickson, R.T. Furnbank, W.S. Chow, A simple alternative approach to assessing the fate of absorbed light energy using chlorophyll fluorescence, *Photosynth. Res.* 82 (2004) 73–81. <https://doi.org/10.1023/B:PRES.0000040446.87305.f4>.
- [51] C. Klughammer, U. Schreiber, Complementary PS II quantum yields calculated from simple fluorescence parameters measured by PAM fluorometry and the saturation pulse method, *PAM Appl* (2008) 27–35, notes 1, <https://walz-usa.com/downloads/pan/PAN078007.pdf>.
- [52] J. Doucha, K. Livansky, Outdoor open thin-layer microalgal photobioreactor: potential productivity, *J. Appl. Phycol.* 21 (2009) 111–117. <https://doi.org/10.1007/s10811-008-9336-2>.
- [53] M. Barceló-Villalobos, J.L. Guzmán Sánchez, I. Martín Cara, J.A. Sánchez Molina, F.G. Ación, Analysis of mass transfer capacity in raceway reactors, *Algal Res.* 35 (2018) 91–97. <https://doi.org/10.1016/j.algal.2018.08.017>.
- [54] A.R. Wellburn, The spectral determination of chlorophylls a and b, as well as total carotenoids, using various solvents with spectrophotometers of different resolution, *J. Plant Physiol.* 144 (3) (1994) 307–313. [https://doi.org/10.1016/S0176-1617\(11\)81192-2](https://doi.org/10.1016/S0176-1617(11)81192-2).
- [55] T.A. Kursar, J. Van der Meer, R.S. Alberty, Light-harvesting system of the red alga *Gracilaria tikvahiae*: I. Biochemical analyses of pigment mutations, *Plant Physiol.* 73 (2) (1983) 353–360. <https://doi.org/10.1104/pp.73.2.353>.
- [56] S.B. Kumar, P. Prabhaskar, A study on starch profile of rajma bean (*Phaseolus vulgaris*) incorporated noodle dough and its functional characteristics, *Food Chem.* 180 (2015) 124–132. <https://doi.org/10.1016/j.foodchem.2015.02.030>.
- [57] S.O. Lourenço, E. Barbarino, P.L. Lavín, U.M. Lanfer Marquez, E. Aidar, Distribution of intracellular nitrogen in marine microalgae: calculation of new nitrogen-to-protein conversion factors, *Eur. J. Phycol.* 39 (2004) 17–32. <https://doi.org/10.1080/0967026032000157156>.
- [58] S.K. Mishra, W.I. Suh, W. Farooq, M. Moon, A. Shrivastav, M.S. Park, J.W. Yang, Rapid quantification of microalgal lipids in aqueous medium by a simple colorimetric method, *Bioresour. Technol.* 155 (2014) 330–333. <https://doi.org/10.1016/j.biortech.2013.12.077>.
- [59] T.A. Rearte, F.L. Figueroa, C. Gómez-Serrano, C.G.S. Vélez, A. Marsili, A. Iorio, C. V. González-López, M.C. Cerón-García, R.T. Abdala-Díaz, F.G. Ación-Fernández, Optimization of the production of lipids and carotenoids in the microalga *Golenkinia aff. brevispicula*, *Algal Res.* 51 (2020), e102004. <https://doi.org/10.1016/j.algal.2020.102004>.
- [60] N.K. Korbee-Peinado, R.T. Abdala-Díaz, F.L. Figueroa, E.W. Helbling, Ammonium and UV radiation stimulate the accumulation of mycosporine-like amino acids in *Porphyra columbina* (Rhodophyta) from Patagonia, Argentina 1, *J. Phycol.* 40 (2) (2004) 248–259. <https://doi.org/10.1046/j.1529-8817.2004.03013.x>.
- [61] R. Re, N. Pellegrini, A. Proteggente, A. Pannala, M. Yang, C. Rice-Evans, Antioxidant activity applying an improved ABTS radical cation decolorization assay, *Free Radic. Biol. Med.* 26 (9–10) (1999) 1231–1237. [https://doi.org/10.1016/S0891-5849\(98\)00315-3](https://doi.org/10.1016/S0891-5849(98)00315-3).
- [62] T. Underwood, Experiments in Ecology. Their Logical Design and Interpretation Using Analysis of Variance, Cambridge University Press, Cambridge UK, 1997.
- [63] M.J. Anderson, R.N. Gorley, K.R. Clarke, PERMANOVA+ for PRIMER: Guide to Software and Statistical Methods, PRIMER-E, Plymouth, UK, 2008.
- [64] A.A. Issa, M.H. Abd-Alla, T. Ohyama, Nitrogen fixing cyanobacteria: future prospect, in: *Advances in Biology and Ecology of Nitrogen Fixation* 2, 2014, pp. 24–48. <https://doi.org/10.5772/56995>.
- [65] G. Torzillo, L. Giannelli, A.J. Martínez-Roldán, N. Verdona, P. De Filippis, M. Scarsella, M. Bravi, Microalgae culturing in thin-layer photobioreactors, *Chem. Eng. Trans.* 20 (2010) 265–270. <https://doi.org/10.3303/CETI1020045>.
- [66] F.G. Ación-Fernández, J.M. Fernández, J.J. Magán, E. Molina, Production cost of a real microalgae production plant and strategies to reduce it, *Biotechnol. Adv.* 30 (2012) 1344–1353. <https://doi.org/10.1016/j.biotechadv.2012.02.005>.
- [67] B.G. Mitchell, Algorithms for determining the absorption coefficient for aquatic particulates using the quantitative filter technique, in: *Ocean Optics International Society for Optics and Photonics vol. 1302*, 1990, pp. 137–148. <https://doi.org/10.1117/12.21440>.
- [68] S.G.H. Simis, M. Tjeldens, H.L. Hoogveld, H.J. Gons, Optical changes associated with cyanobacterial bloom termination by viral lysis, *J. Plankton Res.* 27 (2005) 937–949. <https://doi.org/10.1093/plankt/fbi068>.
- [69] A. Lehmuskero, M. Skogen Chauton, T. Boström, Light and photosynthetic microalgae: a review of cellular- and molecular-scale optical processes, *Prog. Oceanogr.* 168 (2018). <https://doi.org/10.1016/j.poccean.2018.09.002>.
- [70] W.L. Butler, Absorption of light by turbid materials, *J. Opt. Soc. Am.* 52 (1962) 292. <https://doi.org/10.1364/JOSA.52.000292>.
- [71] M. Kishino, N. Takahashi, Okami, S. Ichimura, Estimation of the spectral absorption coefficients of phytoplankton in the sea, *Bull. Mar. Sci.* 37 (1985) 634–642.
- [72] I. Laurion, F. Blouin, Roy, The quantitative filter technique for measuring phytoplankton absorption: interference by MAAs in the UV waveband, *Limnol. Oceanogr. Methods* 1 (2003) 1–9. <https://doi.org/10.4319/lom.2003.1.1>.
- [73] F.L. Figueroa, R. Conde-Álvarez, J. Bonomi Barufi, P.S.M. Celis-Plá, P. Flores, E.-J. Malta, D.B. Stengel, O. Meyerhoff, A. Perez-Ruzafa, Monitoring of effective quantum yield in *Ulva rigida* submitted to different CO₂, nutrient and temperature regimes in outdoor mesocosms, *Aquat. Biol.* 22 (2014) 195–212. <https://doi.org/10.3354/ab00593>.
- [74] F.L. Figueroa, J. Bonomi-Barufi, P.S.M. Celis-Plá, U. Nitschke, F. Arenas, S. Connan, M.T. Mata, D. Meyerhoff, D. Robledo, D. Stengel, Short-term effects of increased CO₂, nitrate, and temperature on photosynthetic activity in *Ulva rigida* (Chlorophyta) estimated by different pulse amplitude modulated fluorometers and oxygen evolution, *J. Exp. Bot.* 72 (2) (2021) 491–509. <https://doi.org/10.1093/jxb/b3/eraa473>.
- [75] J. Lívanský, F. Doucha, CO₂ and O₂ gas exchange in outdoor thin-layer high density microalgal cultures, *J. Appl. Phycol.* 8 (1996) 353–358. <https://doi.org/10.1007/BF02178578>.
- [76] F. Doucha, K. Straka, J. Lívanský, Utilization of flue gas for cultivation of microalgae (*Chlorella* sp.) in an outdoor open thin-layer photobioreactor, *J. Appl. Phycol.* 17 (2005) 403–412. <https://doi.org/10.1007/s10811-005-8701-7>.
- [77] L. Mendez, A. Mahdy, M. Ballesteros, C. González-Fernández, *Chlorella vulgaris* vs cyanobacterial biomasses: comparison in terms of biomass productivity and biogas yield, *Energy Convers. Manag.* 92 (2015) 137–142. <https://doi.org/10.1016/j.enconman.2014.11.050>.
- [78] A. Rearte, P.S.M. Celis-Plá, A. Neori, J. Masojídek, G. Torzillo, C. Gómez, A. M. Silva Benavides, F. Álvarez-Gómez, R. Abdala-Díaz, K. Rangelová, M. Caporgno, T.F. Massocato, J. Carmo da Silva, H. Al-Mahrouqi, R. Atzmüller, F.L. Figueroa, Diurnal changes of dissolved oxygen gradients in the highly productive strain *Chlorella vulgaris* R117 cultured in thin-layer cascades: effect on photosynthetic activity, *Algal Res.* 54 (2021). <https://doi.org/10.1016/j.algal.2020.102176> this issue.
- [79] T. Sakamoto, T. Yoshida, H. Arima, Y. Hatanaka, Y. Takani, Y. Tamaru, Accumulation of trehalose in response to desiccation and salt stress in the terrestrial cyanobacterium *Nostoc commune*, *Phycol. Res.* 57 (2009) 66–73. <https://doi.org/10.1111/j.1440-1835.2008.00522.x>.

- [80] H. Wang, S.J. Wu, D. Liu, Preparation of polysaccharides from cyanobacteria *Nostoc commune* and their antioxidant activities, *Carbohydr. Polym.* 99 (2014) 553–555. <https://doi.org/10.1016/j.carbpol.2013.08.066>.
- [81] P. Pospíšil, A. Arató, A. Krieger-Liszkay, A.W. Rutherford, Hydroxyl radical generation by photosystem II, *Biochemistry* 43 (21) (2004) 6783–6792. <https://doi.org/10.1021/bi036219i>.
- [82] F.R. Conde, M.S. Churio, C.M. Previtali, The deactivation pathways of the excited-states of the mycosporine-like amino acids shinorine and porphyra-334 in aqueous solution, *Photochem. Photobiol. Sci.* 3 (2004) 960–967. <https://doi.org/10.1039/B405782A>.
- [83] W.C. Dunlap, Y. Yamamoto, Small-molecule antioxidants in marine organisms: antioxidant activity of mycosporine-glycine, *Comp. Biochem. Physiol.* 112 (1) (1995) 105–114. [https://doi.org/10.1016/0305-0491\(95\)00086-N](https://doi.org/10.1016/0305-0491(95)00086-N).
- [84] S.P. Singh, R.P. Sinha, M. Klisch, D.P. Häder, Mycosporine-like amino acids (MAAs) profile of a rice-field cyanobacterium *Anabaena doliolum* as influenced by PAR and UVR, *Planta* 229 (1) (2008) 225–233. <https://doi.org/10.1007/s00425-008-0822-1>.
- [85] J. Doucha, K. Lfvanský, Productivity, CO₂/O₂ exchange and hydraulics in outdoor open high density microalgal (*Chlorella* sp.) photobioreactors operated in a Middle and Southern European climate, *J. Appl. Phycol.* 18 (6) (2006) 811–826.